Journal of Medicinal Chemistry

Article

pubs.acs.org/jmc

Structure-Based Discovery of Novel Cyclophilin A Inhibitors for the Treatment of Hepatitis C Virus Infections

Suhui Yang,[†,∇,○] Jyothi K.R.,[‡,○] Sangbin Lim,[‡] Tae Gyu Choi,[‡] Jin-Hwan Kim,[‡] Salima Akter,[‡] Miran Jang,[‡] Hyun-Jong Ahn,[§] Hee-Young Kim,[∥] Marc P. Windisch,[∥] Daulat B. Khadka,[†] Chao Zhao,[†] Yifeng Jin,[†] Insug Kang,[‡] Joohun Ha,[‡] Byung-Chul Oh,[⊥] Meehyein Kim,[#] Sung Soo Kim,[*,‡] and Won-Jea Cho[*,†]

[†]College of Pharmacy and Research Institute of Drug Development, Chonnam National University, Gwangju 500-757, Republic of Korea

[‡]Department of Biochemistry and Molecular Biology, School of Medicine, Kyung Hee University, Seoul 130-701, Republic of Korea

[§]Department of Microbiology, School of Medicine, Kyung Hee University, Seoul 130-701, Republic of Korea

[∥]Applied Molecular Virology, Institute Pasteur Korea, Gyeonggi-do 463-400, Republic of Korea

[⊥]Lee Gil Ya Cancer and Diabetes Institute, Gachon University of Medicine and Science, Incheon 406-840, Republic of Korea

[#]Virus Research and Testing Group, Korea Research Institute of Chemical Technology, Daejeon 305-600, Republic of Korea

Supporting Information

ABSTRACT: Hepatitis C virus (HCV) is a major cause of end-stage liver disease. Direct-acting antivirals (DAAs), including inhibitors of nonstructural proteins (NS3/4A protease, NS5A, and NS5B polymerase), represent key components of anti-HCV treatment, but these are associated with increased drug resistance and toxicity. Thus, the development of host-targeted antiviral agents, such as cyclophilin A inhibitors, is an alternative approach for more effective, selective, and safer treatment. Starting with the discovery of a bis-amide derivative **5** through virtual screening, the lead compound **25** was developed using molecular modeling-based design and systematic exploration of the structure−activity relationship. The lead **25** lacked cytotoxicity, had potent anti-HCV activity, and showed selective and high binding affinity for CypA. Unlike cyclosporin A, **25** lacked immunosuppressive effects, successfully inhibited the HCV replication, restored host immune responses without acute toxicity in vitro and in vivo, and exhibited a high synergistic effect in combination with other drugs. These findings suggest that the bis-amides have significant potential to extend the arsenal of HCV therapeutics.

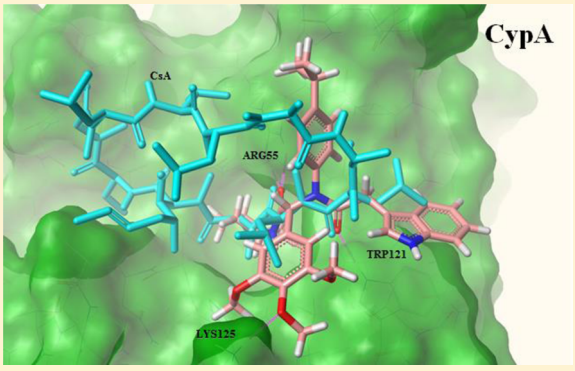

INTRODUCTION

Hepatitis C is an infectious disease affecting primarily the liver and is caused by the hepatitis C virus (HCV). Chronic infection with HCV is a high risk factor for developing serious liver diseases, particularly cirrhosis and hepatocarcinoma.[1] HCV patients were treated with a combination of pegylated interferon α (pegIFN-α) and ribavirin until 2011.[2] A sustained virologic response (SVR) to the treatment or the state of aviremia was achieved in 54−56% of the patients treated.[3,4] Since the approval of the first direct-acting antivirals (DAAs), telaprevir and boceprevir (viral nonstructrural protein, NS3/4A protease, inhibitors), triple combination therapy including DAA became a standard treatment for chronic HCV infection.[5,6] Triple combination therapy regimens demonstrated a notable improvement in cure rates of HCV genotype 1, the most common type.[7,8] Triple combination therapy achieved a SVR in 75% of patients. The SVR increased to >79% when telaprevir or boceprevir were replaced by simeprevir, an NS3/4A protease inhibitor.[9] With the approval of a new combination treatment employing sofosbuvir (NS5B polymerase inhibitor) and ledipasvir (NS5A inhibitor) that achieved >94% SVR in patients with HCV genotype 1 infection, pegIFN-α-free regimens with or without ribavirin have become common for HCV treatment. In addition to these DAAs, ombitasvir (NS5A inhibitor), paritaprevir (NS3/4A protease inhibitor), dasabuvir (NS5B polymerase inhibitor), and daclatasvir (NS5A inhibitor) in pegIFN-α-free regimens have been assessed for the treatment of HCV genotypes 1−6.[10−16]

Although DAAs show potent antiviral activity and acceptable safety profiles, DAA-based treatment regimens have several distinct limitations; these include treatment-emergent viral mutations and drug resistance, cross-resistance between DAAs of the same family, a prevalence of HCV variants with a natural

Received: July 13, 2015

DOI: 10.1021/acs.jmedchem.5b01064
J. Med. Chem. XXXX, XXX, XXX−XXX

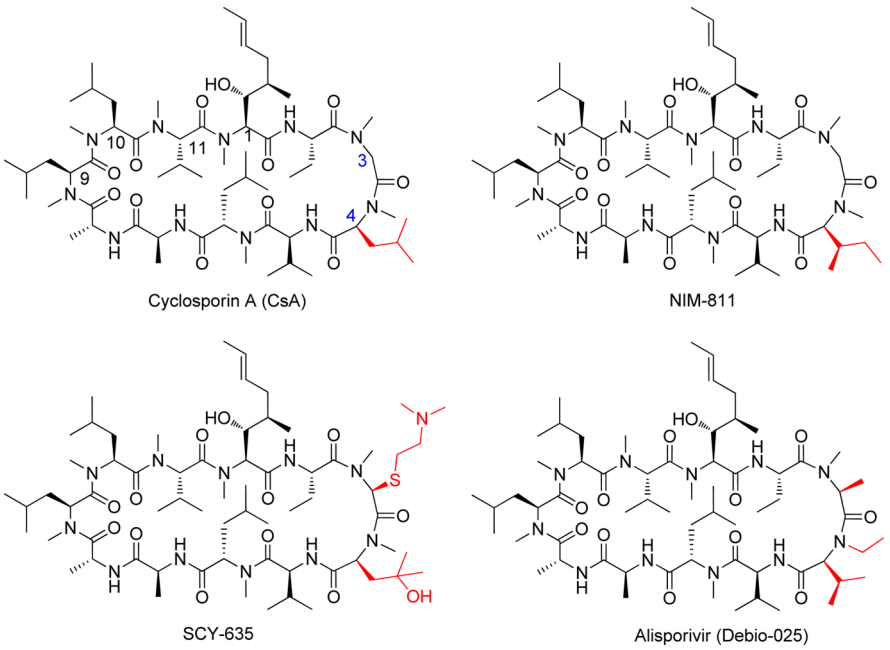

Figure 1. Structures of four CypA inhibitors: CsA, NIM-811, SCY-635, and alisporivir.

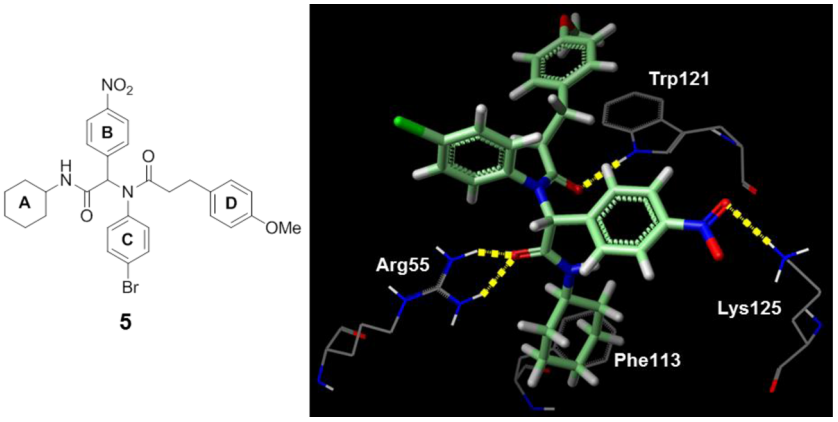

Figure 2. Chemical structure of **5** and its binding mode inside CypA.

polymorphism associated with DAA resistance, and HCV genotype-dependent differences in antiviral activities.[5,17−23] These issues spurred us to develop indirectly acting, host-targeting antiviral drugs such as inhibitors of cyclophilin, which is required for HCV replication. Combination therapy with cyclophilin inhibitors may provide an alternative and complementary strategy with a multigenotypic high barrier of resistance for HCV infection.

Since cyclosporin A (CsA) shows antiviral effects via cyclophilin A (CypA) inhibition, CypA has become a target for HCV treatment (Figure 1).[24] Cyps are a family of highly conserved cellular peptidyl-prolyl cis−trans isomerases (PPIase) and are involved in cellular processes including protein folding and trafficking. CypA is the most abundant family member, and its critical role in supporting HCV-specific RNA replication and viral protein expression has been reported in several studies.[25,26] Though CsA has antiviral efficacy, the CsA-CypA complex also blocks the dephosphorylation-driven nuclear translocation of nuclear factor of activated T cells (NFAT), eventually leading to the clinical use of CsA as an immunosuppressant.[27] Therefore, nonimmunosuppressive CsA analogs, such as NIM-811,[28] SCY-635,[29] and alisporivir (Debio-025),[30] have been developed through chemical modification at either position 3 or 4 of CsA. These analogs have been shown to possess not only potent efficacy against HCV replication but also a long lasting antiviral response and a higher genetic barrier to resistance compared to those of DAAs (Figure 1). However, the clinical safety profile of these inhibitors has yet to be resolved. Besides, CsA-based inhibitors share the same backbone scaffold and may possibly have broad specificity to Cyp isoforms. Taking into consideration the potential limitations of CsA-based inhibitors and the strong involvement of CypA in HCV replication, we herein report the identification and development of a novel series of potent and selective CypA inhibitors as anti-HCV agents.

RESULTS AND DISCUSSION

As the conserved amino acid residues making up the catalytically active site for the PPIase domain of CypA were identified,[31,32] we searched for compounds targeting this region in order to attain a high specificity for CypA. Over 200 000 compounds were screened for their binding affinity for the

DOI: 10.1021/acs.jmedchem.5b01064
J. Med. Chem. XXXX, XXX, XXX−XXX

ligand binding domain (LBD) of the CsA-CypA complex (PDB code 1CWA) to discover potential inhibitors of CypA PPIase activity (Figure S1).[33] The binding affinities were predicted based on five different scoring functions and consensus scores by applying Surflex-Dock. Of the high scoring compounds, **5** emerged as a promising hit (Figure 2). The computational binding mode of **5** with CypA shows that the carbonyl oxygen of two amides and the nitro group of the ring (B) of the bis-amide interact with the amino acid residues Arg55, Trp121, and Lys125 of CypA through H-bonds. A hydrophobic interaction is observed between the cyclohexyl ring (A) and Phe113. However, the phenylethyl moiety (D) is entirely devoid of chemical interactions; the moiety projects outward from the protein core and lacks contact with any amino acid. Thus, we reasoned that modification of the flexible phenylethyl group to a constrained indolylmethyl or a phenyl moiety might be advantageous, since this modification would place the rigid aromatic ring over the indole of Trp121 to establish a $\pi-\pi$ stacking interaction.

Various novel analogs of bis-amide **5** were prepared by employing Ugi multicomponent reaction as extension of the Passerini three-component reaction.[34,35] In general, Ugi four-component condensation involves the in situ formation of an imine from an aldehyde **2** and an amine **3**. The subsequent reaction of the imine with carboxylic acid **4** and an isocyanide **1** produces an intermediate, which rearranges via an acyl transfer to yield the bis-amides (Scheme 1). The Ugi multicomponent

Scheme 1. Synthesis of Bis-amides 5−25[a]

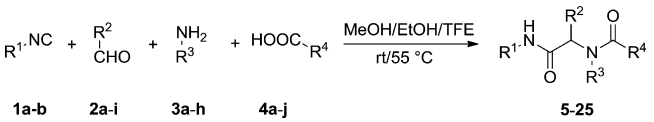

1a-b 2a-i 3a-h 4a-j 5-25

[a]Isocyanides **1**, aldehydes **2**, amines **3**, and carboxylic acids **4** are listed in Table S1.

reaction offers the major advantage that most Ugi products can be isolated as solids without the need for further purification steps, which saves time and effort.[35] Therefore, this reaction type is a highly efficient method for creating molecular diversity in a single reaction vessel. Prior to synthesis, we investigated the effect of several reaction parameters including temperature, solvent, and microwave irradiation (Tables S2 and S3). On the basis of these findings, a total of 21 bis-amides (**5−25**) were prepared by the Ugi reaction using the polar protic solvents such as methanol, ethanol, or 2,2,2-trifluoroethanol (TFE) at room temperature or at 55 °C (Scheme 1 and Table 1).

The newly synthesized bis-amide analogs were initially screened for their effect on the viability of mock-infected and chemical-treated Huh7.5 cells and for their anti-HCV activity (Table 1).[36−38] The antiviral activity of the hit **5** (half maximal effective concentration EC_{50} = 6.1 ± 4.7 μM) was similar to that of IFN-α (EC_{50} = 6.2 ± 1.6 μM). Furthermore, the derivatives **6** (EC_{50} = 3.3 μM) and **7** (EC_{50} = 2.5 ± 0.1 μM) displayed even more potent antiviral activities. However, these compounds were cytotoxic (half maximal cytotoxic concentration $CC_{50} \leq 10$ μM). Bis-amides **8−13** were less cytotoxic (CC_{50} > 22 μM) but showed lower antiviral activities, with EC_{50} values that were greater than their CC_{50} values. Derivatives **14−18** were not cytotoxic (CC_{50} > 36 μM) and displayed low to moderate antiviral effects (selectivity index [SI, CC_{50}/EC_{50}]: 1.8−3.3). Analogs **19−22** were even less cytotoxic (CC_{50} > 64 μM) and displayed potent anti-HCV activity (SI: 6.1−9.6). Bis-amides **23−25** were the most active compounds in the series. They displayed no apparent cytotoxicity and had potent anti-HCV activity, with SI values of >11.2, >13.8, and >19.2 for **23**, **24**, and **25**, respectively; these compared favorably to those of ribavirin (SI > 6.1) and INF-α (SI > 16.1).

The cytotoxicity and anti-HCV activity of bis-amides were dependent upon the isocyanide, aldehyde, amine, and carboxylic acid used for the synthesis (Table 1). For a preliminary structure−activity relationship study, 13 bis-amides (**6**, **7**, **14**, **15**, and **17−25**) that had SI values greater than 2 were considered. Their antiviral effects seemed to vary greatly, depending on the substituent of the phenyl ring at the R^2 position. Bis-amide **6**, with a chlorine group at the para position of the phenyl moiety, showed about 5-fold stronger anti-HCV activity than compound **14**, with trimethoxy substituents. Furthermore, the antiviral activity of bis-amide **7**, with a nitro group, was 10-fold greater than that of compound **18**, with a fluorine group. In fact, bis-amide **7** showed the most potent anti-HCV activity (EC_{50} = 2.5 ± 0.1 μM). The potent antiviral activity of bis-amide **7** indicates that the NO_2 of this compound orients in similar direction as that of the hit compound **5**, to interact with Lys125 of CypA.

Varying the substitution on the phenyl ring at the R^3 position also had a significant impact on compound cytotoxicity and anti-HCV activity. Introduction of a para isopropyl substituent on the phenyl ring (**25**) led to a 3-fold increase in antiviral activity, as compared to **14**; interestingly, compound **25** was noncytotoxic, resulting in a remarkable increase in SI (>19.2). Furthermore, modification at the R^4 position produced variable effects on cytotoxicity and anti-HCV activity. The dimethyl-phenyl substituted compound **19** had a slightly more active anti-HCV activity (about 1.3-fold) than the bis-amide **15**, with a meta methoxyphenylethyl moiety. Comparison of the structures of **17** and **23** showed that the anti-HCV activity of the nonsubstituted phenyl ring at R^4 (**23**) was about 4-fold greater than that of the substituted ring (**17**). Moreover, replacement of the phenyl ring (**20**) by a methyl substitution (**21**) at R^4 was also favorable and produced a slight (1.5-fold) increase in anti-HCV activity.

Taken together, four bis-amides (**6**, **7**, **20**, and **25**) exhibited low micromolar EC_{50} values that were similar to or greater than those of the hit compound **5**, ribavirin, and INF-α. Among these compounds, the bis-amide **25** seemed to be optimal for further studies because of its low cytotoxicity (CC_{50}). Moreover, investigation of the inhibitory effect of the hit **5** and the bis-amide **25** on CypA PPIase activity revealed that compound **25** produced a substantial low-nanomolar inhibition effect (IC_{50} = 5.5 nM), which was greater than that of the hit **5** (IC_{50} = 11.2 nM). Thus, in view of its low cytotoxicity, potent anti-HCV effect, and effective inhibition of CypA PPIase activity, the bis-amide **25** was selected as a lead novel CypA inhibitor.

Similar to that of the hit **5**, the hydrophobic interaction between Phe113 of CypA and the cyclohexyl ring (A) of **25** remained intact (Figure 3A and S2). Bis-amide **25** strongly interacted with Arg55, Trp121, and Lys125 of CypA through 4 H-bonds by an oxygen atom of trimethoxyphenyl (B) and each carbonyl oxygen from two amides. The branched isopropyl group (C) was more likely to fit into the hydrophobic region of the intact vicinity than that observed for the bromo group of the hit **5**. Rigidification of the phenylethyl group to the indolylmethyl moiety (D) appeared to generate a $\pi-\pi$

DOI: 10.1021/acs.jmedchem.5b01064
J. Med. Chem. XXXX, XXX, XXX−XXX

Table 1. Cytotoxicity and Anti-HCV Activity of the Bis-amides 5−25

Compd	R^1	R^2	R^3	R^4	CC_{50}[a] (μM)	EC_{50}[b] (μM)	SI[c]
5					9.8 ± 0.0	6.1 ± 4.7	1.6
6					10.2 ± 0.2	3.3	3.1
7					8.5 ± 0.2	2.5 ± 0.1	3.4
8					30.5 ± 3.9	>30.5	-[d]
9					23.2 ± 1.1	>23.2	-[d]
10					27.1 ± 0.2	>27.1	-[d]
11	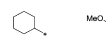				>100.0	>100.0	-[d]
12					22.5 ± 0.1	>22.3	-[d]
13					32.2 ± 1.5	>32.2	-[d]
14					36.8 ± 2.6	16.3 ± 2.4	2.2
15					51.5 ± 4.8	15.5 ± 0.6	3.3
16					57.4 ± 3.5	31.1	1.8
17					>100	34.8 ± 12.9	>2.8
18					63.6 ± 1.1	26.5 ± 15.6	2.4
19					69.8 ± 4.6	11.4 ± 7.3	6.1
20					64.5 ± 3.2	6.7 ± 0.4	9.6
21					89.2 ± 15.3	10.8 ±0.8	8.2
22					68.3 ± 1.4	7.9 ± 0.9	8.6
23					>100	8.9 ± 3.4	>11.2
24					>100	7.2 ± 0.9	>13.8
25					>100	5.2 ± 0.7	>19.2
Ribavirin	-	-	-	-	>100	16.3 ± 3.0	>6.1
INF-α	-	-	-	-	>100	6.2 ± 1.6	>16.1

[a]CC_{50}: half maximal cytotoxic concentration. [b]EC_{50}: half maximal effective concentration. [c]SI: selectivity index (CC_{50}/EC_{50}). [d]Not active.

interaction with Trp121 as expected. The binding mode of the **25** was consistent with that of the proposed mechanism. The binding mode was further supported by the potent antiviral activity of bis-amides **20** and **21**, with an isopropyl phenyl ring (C), and compounds **19**, **20**, and **22**−**24**, with a rigid aromatic ring (D).

Next, surface plasmon resonance (SPR) was used to evaluate the binding affinity of **25** for CypA. Bis-amide **25** had a slower dissociation rate from CypA (K_{on} = 8.1 × 10^3 M^{-1} s^{-1}, K_{off} = 6.0 × 10^{-4} s^{-1}) than that of CsA (K_{on} = 7.6 × 10^3 M^{-1} s^{-1}, K_{off} = 2.5 × 10^{-2} s^{-1}), indicating stronger affinity of **25** for CypA compared to that of CsA (Figure 3B, upper panel). But the dissociation rates of **25** and CsA for CypB reversed (Figure 3B, lower panel). Intriguingly, the dissociation constant (K_D) calculated from SPR-based kinetic analysis indicated a much stronger binding affinity of **25** for CypA (K_D = 570 ± 20 nM) than for CypB (K_D = 2.1 ± 4 μM), confirming its selectivity for CypA (Figure 3C). To further confirm the binding affinity of **25** and the associated thermodynamic properties, isothermal titration calorimetry (ITC)[39] was performed, and a reasonable fit with a two-site set model was achieved (Figure S3 and Table S4). In addition, the enzyme kinetic studies illustrated that the CypA PPIase activity inhibition by **25** (IC_{50} of 5.5 ± 1.6 nM) was about 1.3-fold greater than that of CsA (IC_{50} of 7.2 ± 1.7 nM) (Figure S4). Its strong binding affinity and anti-PPIase activity highly suggest that **25** is a potent and selective CypA inhibitor.

Antigens activate immune cells by increasing the level of intracellular Ca^{2+}, causing the activation of the calmodulin-dependent phosphatase calcineurin. Subsequently, calcineurin dephosphorylates NFAT, resulting in translocation of NFAT to the nucleus and the induction of interleukin 2 (IL-2) secretion.[40] Since the adaptive immune response is essential to eradication of HCV, CsA, a well-known immunosuppressant, cannot be used as an anti-HCV agent, spurring the development of nonimmunosuppressive CsA analogs.[41] To verify **25** as a nonimmunosuppressive CypA inhibitor, we explored its effect on the calcineurin/NFAT/IL-2 signaling pathway in ionophore-stimulated mouse splenocytes. Unlike CsA, **25** neither was cytotoxic (Figure 4A) nor inhibited calcineurin phosphatase activity (Figure 4B). Moreover, **25** maintained the dephosphorylated state of NFAT1 (Figure 4C), allowing for nuclear translocation of NFAT1 (Figure 4D) and, consequently, constant IL-2 production. On the other hand, CsA profoundly blocked IL-2 secretion as previously described by others (Figure 4E).[42]

It is known that disruption of CypA interaction with viral proteins results in formation of an ineffective replication complex and a significant decrease in viral RNA synthesis.[43,44] We found that **25** efficiently reduced HCV RNA replication levels (Figure 5A), and the expression of the viral proteins NS5A and NS5B in total cell lysates (Figure 5B) and membrane fractions (Figure 5C). The decrease in NS5A and NS5B levels was further confirmed by confocal microscopy studies (Figure 5D). Importantly, the reduced CypA level in

DOI: 10.1021/acs.jmedchem.5b01064
J. Med. Chem. XXXX, XXX, XXX−XXX

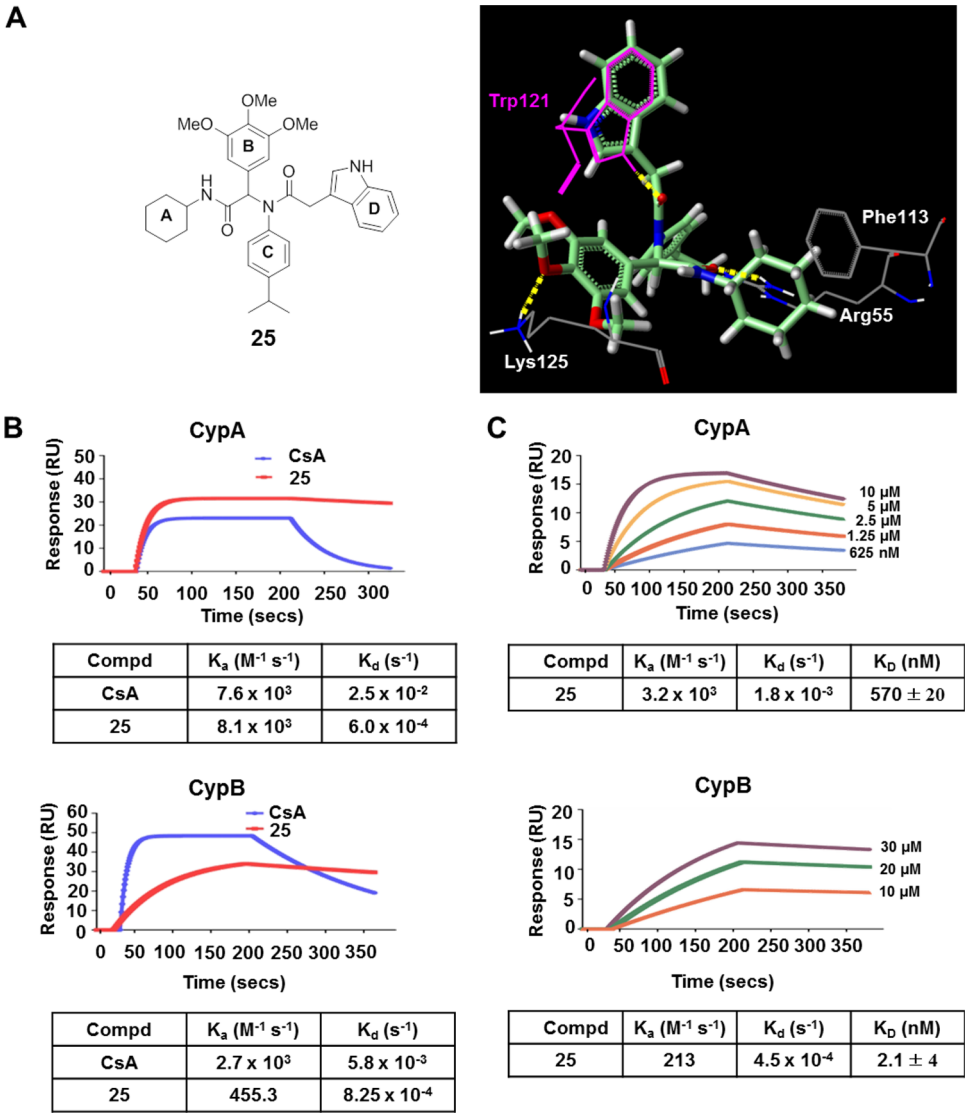

Compd	K_a (M^{-1} s^{-1})	K_d (s^{-1})
CsA	7.6 x 10^3	2.5 x 10^{-2}
25	8.1 x 10^3	6.0 x 10^{-4}

Compd	K_a (M^{-1} s^{-1})	K_d (s^{-1})	K_D (nM)
25	3.2 x 10^3	1.8 x 10^{-3}	570 ± 20

Compd	K_a (M^{-1} s^{-1})	K_d (s^{-1})
CsA	2.7 x 10^3	5.8 x 10^{-3}
25	455.3	8.25 x 10^{-4}

Compd	K_a (M^{-1} s^{-1})	K_d (s^{-1})	K_D (nM)
25	213	4.5 x 10^{-4}	2.1 ± 4

Figure 3. (A) Chemical structure of **25** and its binding mode. (B) Sensograms showing **25** and CsA binding to CypA and CypB (upper and lower panels, respectively). (C) Relative response in resonance units showing interactions of **25** with CypA and CypB (upper and lower panels, respectively) at the different concentrations indicated. The K_D values (±sd) were calculated from three independent experiments.

the membrane fraction without a change in the total protein level suggested that **25** blocked recruitment of CypA to the membrane to form the replication complex. The lead **25** also prevented the binding of CypA to NS5A and NS5B (Figure S5). Furthermore, **25** exhibited potent antiviral activity in Con1b (genotype 1b) and JFH1 (genotype 2a) replicon cells with low cytotoxicity (Figure 5E and Figure 5F). These results provide strong evidence that **25** possesses potent antiviral activity by disturbing the interaction of CypA with viral proteins and thus suppresses CypA PPIase activity to prevent HCV replication.

CypA inhibitors are also known to exert antiviral activity by modulating the host cell's innate immune response via IFN-α,[45] whose production is reduced by HCV via the Janus kinase-signal transducer and activator of transcription (JAK-STAT) pathway.[46] In fact, HCV upregulates IL-8 expression, which reduces the induction of IFN-stimulated genes (ISGs) triggered by IFN-α. This is demonstrated in HCV patients that show increased levels of serum IL-8.[47] The lead **25** stimulated the expression of IFN-α signaling molecules (Figure 6A and Figure 6B) but strongly reduced the mRNA and protein levels of IL-8 (Figure 6C and Figure 6D) in a time-dependent manner. It also upregulated IFN-α mRNA (Figure 6E) and protein levels (Figure 6F) in HCV replicon cells. To combat the high rate of emerging viral resistance, a combination of multiple drugs, each with a different mechanism of action, is of utmost importance. For example, the combination of CypA inhibitors with IFN-α resulted in a higher antiviral response than that observed for IFN-α alone.[48] Next, we measured the antiviral effects of **25** combined with IFN-α, ribavirin, or telaprevir. Combination of **25** with each antiviral agent displayed a notable synergistic inhibition on HCV-specific RNA and IL-8 levels compared to CsA-drug combinations (Figure 7A and Figure 7B). Furthermore, the treatment of **25** combined with each agent such as IFN-α, ribavirin, or telaprevir showed no or little cytotoxicity, in contrast to that observed for the CsA-drug combinations (about 20−40% cell death, Figure 7C). Taken together, **25** restores the innate antiviral response by suppressing IL-8 levels and inducing IFN-α production and

DOI: 10.1021/acs.jmedchem.5b01064
J. Med. Chem. XXXX, XXX, XXX−XXX

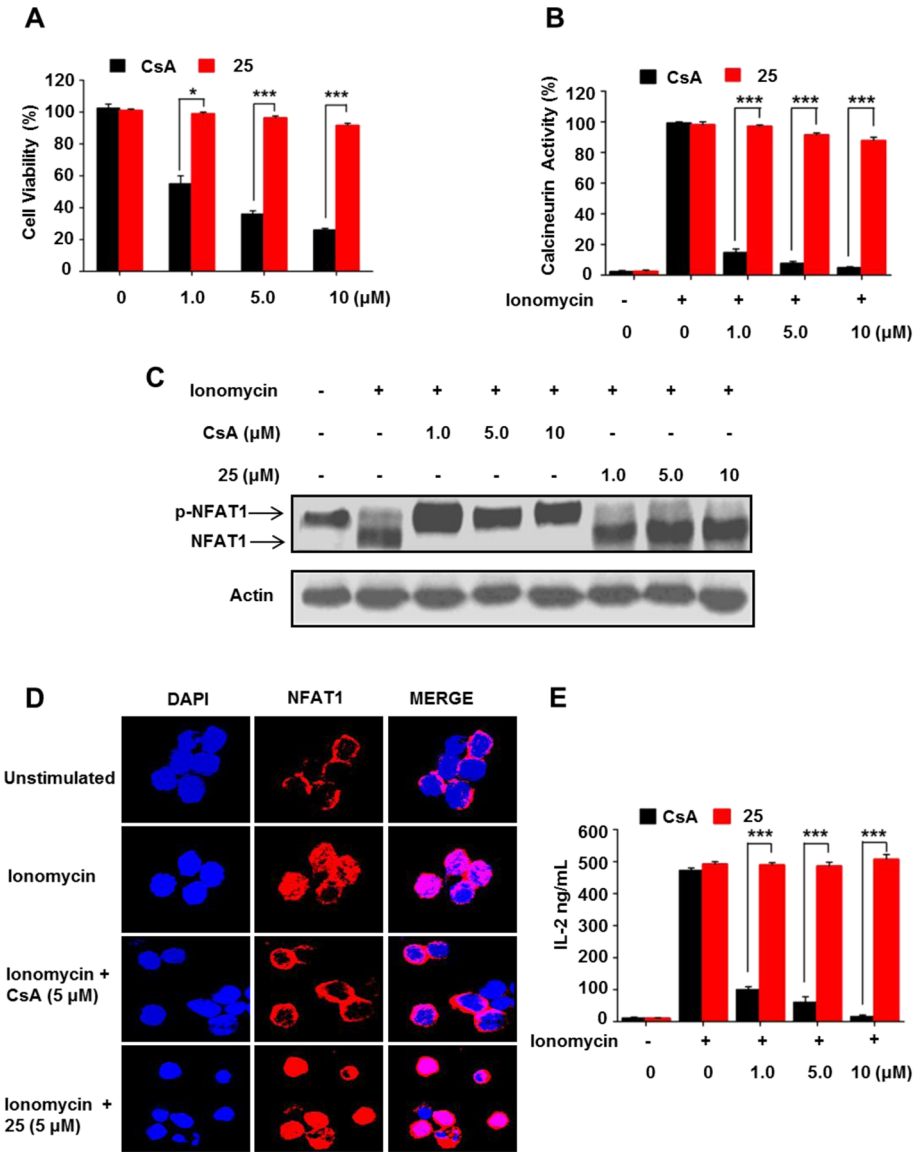

Figure 4. Nonimmunosuppressive activity of **25**: effects of CsA and **25** on (A) mouse splenocyte viability, (B) calcineurin phosphatase activity, (C) phosphorylation of NFAT1, (D) nuclear translocation of NFAT1, and (E) IL-2 production. All data are representative of at least three different experiments.

may prove to be a new valuable drug in anti-HCV combination therapy.

To explore the in vivo antiviral effect of **25**, we engrafted immunodeficient NOD/SCID mice with control Huh7 cells or Huh7 cells containing the HCV-Con1b replicon by intrasplenic injection.[49] Six weeks after the cell transplantation, two groups of five mice were treated with CsA or **25** for 2 weeks (Figure 8A). The liver-engrafted cells were analyzed using hematoxylin and eosin (H&E) staining (Figure 8B). Mice treated with **25** showed no change in body weight, contrary to CsA-treated mice (Figure 8C). Importantly, HCV RNA levels were lower in the **25**-treated mice compared to that in the CsA-treated mice (Figure 8D). Furthermore, Western blot and confocal microscopy analysis showed that **25** strongly inhibited NS5A and NS5B protein levels in the mouse liver tissue (Figure 8E and Figure 8F). Intriguingly, the in vivo acute toxicity assay using BALB/c mice showed that **25** did not affect the body weight or serum hepatic enzyme and creatinine levels remarkably, indicating that **25** did not cause hepatotoxicity or nephrotoxicity (Figure S6).

CONCLUSION

We identified bis-amides as novel CypA inhibitors through virtual screening. To our knowledge, this is the first report on bis-amides as enzymatically active, site-directed inhibitors of CypA. The lead **25** is a selective, nonimmunosuppressive, and potent CypA inhibitor with a structure highly distinct from that of CsA-based inhibitors, showing higher binding affinity, CypA specificity, and stronger anti-PPIase activity compared to those of CsA. It also effectively reduced HCV replication without acute toxicity in vitro and in vivo through the direct inhibition of viral proteins. Furthermore, this inhibition contributed to the reactivation of the host immune response. The combination of **25** with other antiviral agents resulted in a strong synergistic therapeutic activity compared to that of monotherapy or to that of CsA-drug combinations. On the basis of these findings, we

DOI: 10.1021/acs.jmedchem.5b01064
J. Med. Chem. XXXX, XXX, XXX−XXX

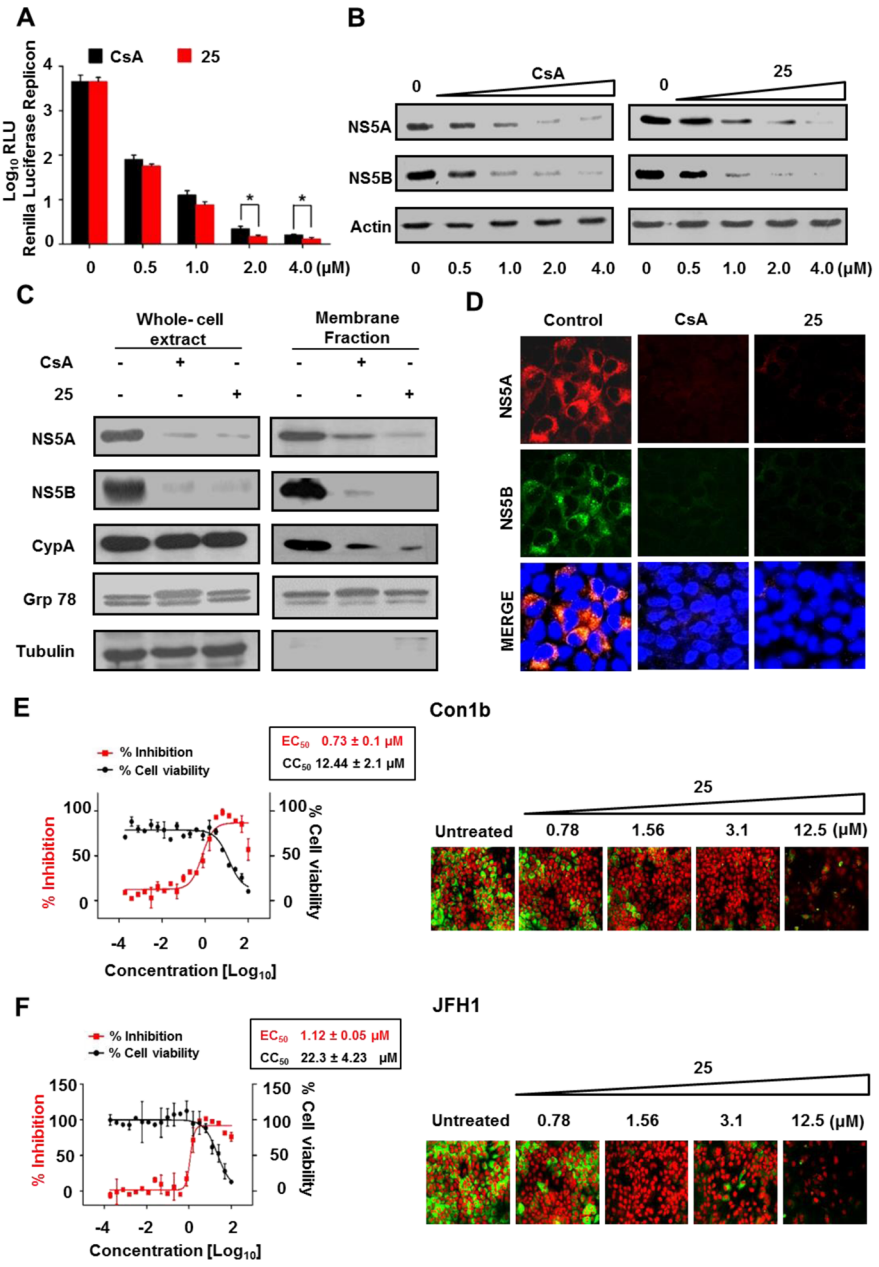

Figure 5. Effect of **25** in HCV replicon cells. (A) HCV RNA levels at increasing concentrations of CsA and **25**. (B) Western blot analysis. HCV replicon cells were treated with increasing concentrations of CsA or **25** and were analyzed for NS5A (upper panels) and NS5B (middle panels) expression. All data are representative of at least three different experiments. (C) HCV Con1b replicon cells were treated with 2 μM CsA or **25**, and the total lysates and subcellular fractionated membranes were used to analyze the replication complex. (D) Confocal microscopy images. The cells were stained with an Alexa red- and Alexa green-conjugated antibody against NS5A and NS5B, respectively, and with DAPI for nuclear staining. Colocalization of merged red and green colors are shown in yellow. The images are representative of at least three different experiments. (E) Real-time image analysis. The potency of **25** was determined by the percentage of fluorescent cells in each image using subgenotype 1b replicon cells. The EC_{50} and CC_{50} were calculated by nonlinear regression analysis using GraphPad Prism (GraphPad Software, Inc., La Jolla, CA, USA). Shown is quantification of the GFP expression levels (left panel). GFP images of replicon levels were acquired at increasing concentrations of **25** (right panel). (F) Same as part E except for the use of JFH1 genotype 2a replicon cells.

believe that **25** may be a promising host-targeted anti-HCV drug in the next generation of combinatorial HCV treatments.

EXPERIMENTAL SECTION

Chemistry. Melting points were determined by the capillary method with a MEL-TEMP capillary melting point apparatus and were uncorrected. IR spectra were obtained on a JASCO FT/IR 300E Fourier transform infrared spectrometer using KBr pellets. ^{1}H NMR, ^{13}C NMR, ^{1}H–^{1}H COSY, and HSQC spectra were recorded with Varian Unity Plus 300 MHz, Varian Unity Inova 500 MHz, and Varian VNMRS 600 MHz spectrometers at the Korea Basic Science Institute. The chemical shifts are reported in ppm downfield to TMS (δ = 0). The coupling constant (J) is shown in Hz. The data are reported in the following order: chemical shift, multiplicity (s, singlet; bs, broad singlet; b, broad; d, doublet; t, triplet; q, quartet; m, multiplet; dd, double doublet), coupling constant, and number of protons. Mass spectra were obtained on a Shimadzu LCMS-2010 EV liquid chromatograph mass spectrometer using the electron spray ionization (ESI) method. HRMS results were obtained on a Waters Synapt G2

DOI: 10.1021/acs.jmedchem.5b01064
J. Med. Chem. XXXX, XXX, XXX−XXX

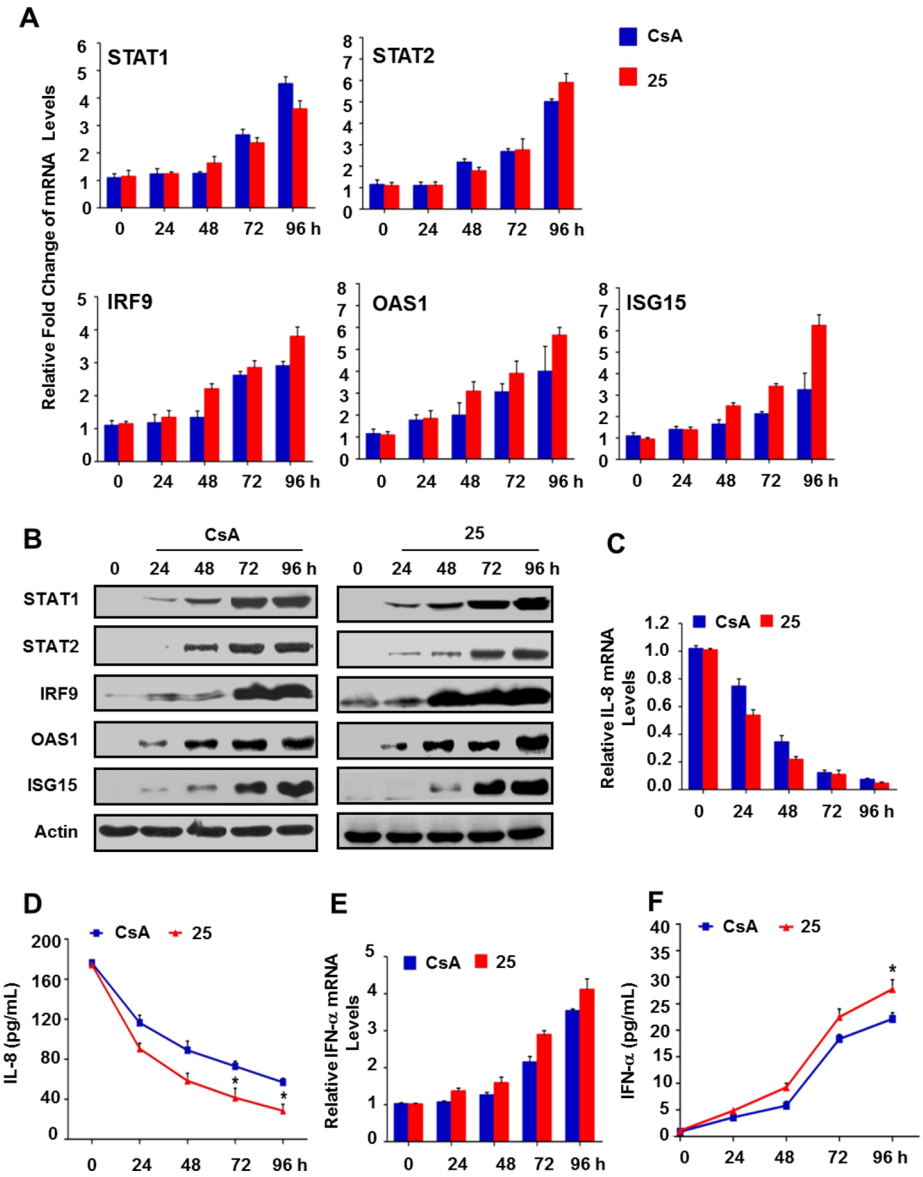

Figure 6. Lead **25** stimulates IFN signals and inhibits IL-8 production in HCV replicon cells. (A) Real time qRT-PCR analysis with 2 μM CsA or **25** at different time intervals. (B) Western blot analysis with the indicated antibodies. (C) Same as part A except that changes in the IL-8 mRNA expression were analyzed. (D) ELISA analysis of the IL-8 levels. (E) Real time qRT-PCR analysis of IFN-α. The results were normalized to human glyceraldehyde 3-phosphate dehydrogenase (GAPDH). (F) ELISA analysis of IFN-α secretion in the culture media. All data are representative of three different experiments.

high definition mass spectrometer. Elemental analyses were performed using the Thermo Fisher Flash 2000 elemental analyzer, and the values obtained were within ±0.4% of the theoretical values. The purity of the compounds was determined by HPLC. The purity was established by integration of the areas of all peaks detected and was reported for each final compound. The specifications of the HPLC analysis were as follows: column, ACE 5 C18-HL, 250 mm × 2.1 mm id; flow rate, 0.2 mL/min; mobile phase, acetonitrile/water = 9:1. Column chromatography (gravity) and medium performance liquid chromatography (MPLC, flow rate, 10 mL/min; make, Yamazen) were performed with a Merck silica gel 60 (70−230 mesh). TLC was performed using plates coated with silica gel 60 F_{254} (Merck). All chemical reagents were purchased from Sigma-Aldrich and Tokyo Chemical Industry Co., Ltd., Japan, and were used without further purification. The solvents were distilled prior to use. All reactions were conducted in oven-dried glassware with magnetic stirring.

***N*-(4-Bromophenyl)-*N*-[cyclohexylcarbamoyl-(4-nitrophenyl)methyl]-3-(4-methoxyphenyl)propionamide (5).** A mixture of 4-nitrobenzaldehyde **2a** (100 mg, 0.66 mmol) and 4-bromoaniline **3a** (141 mg, 0.82 mmol) in methanol was stirred overnight at rt. Cyclohexyl isocyanide **1a** (72 mg, 0.66 mmol) and 3-(4-methoxyphenyl)propionic acid **4a** (180 mg, 1.00 mmol) were added to the mixture. The resulting reaction mixture was stirred at rt. The precipitate thus obtained was filtered off to obtain **5** as a light yellow solid (128 mg, 32%). Mp: 255.2−265.8 °C (decomposed). IR (cm^{-1}): 3269, 1646. ^{1}H NMR (300 MHz, $CDCl_3$) δ: 8.34 (d, J = 8.7 Hz, 2H), 8.06 (t, J = 9.0 Hz, 4H), 7.14 (d, J = 8.4 Hz, 2H), 6.97 (d, J = 8.7 Hz, 2H), 6.78 (d, J = 8.7 Hz, 2H), 6.06 (s, 1H), 5.76 (d, J = 8.4 Hz, 1H), 3.85−3.77 (m, 4H), 2.85 (t, J = 7.5 Hz, 2H), 2.34−2.28 (m, 2H), 1.96−1.82 (m, 2H), 1.73−1.64 (m, 3H), 1.39−1.32 (m, 2H), 1.19−1.02 (m, 3H). ^{13}C NMR (125 MHz, DMSO-d_6) δ: 171.1, 167.5, 157.5, 146.7, 143.2, 141.3, 138.7, 132.9, 132.7, 132.2, 131.1, 129.8, 129.1, 124.0, 123.5, 123.0, 113.7, 54.9, 47.9, 36.6, 32.1, 29.8, 25.1, 24.5, 24.4. MS (ESI) m/z: 592 $(M - H)^-$. HRMS (ESI) m/z: 618.1404 $(M + Na)^+$ (calcd for $C_{30}H_{32}{}^{81}BrN_3NaO_5$, 618.1403), 616.1419 $(M + Na)^+$ (calcd for $C_{30}H_{32}{}^{79}BrN_3NaO_5$, 616.1423), 596.1582 $(M + H)^+$ (calcd for $C_{30}H_{33}{}^{81}BrN_3O_5$, 596.1583), 594.1601 $(M + H)^+$ (calcd for $C_{30}H_{33}{}^{79}BrN_3O_5$, 594.1604). HPLC: purity 97.5%.

DOI: 10.1021/acs.jmedchem.5b01064
J. Med. Chem. XXXX, XXX, XXX−XXX

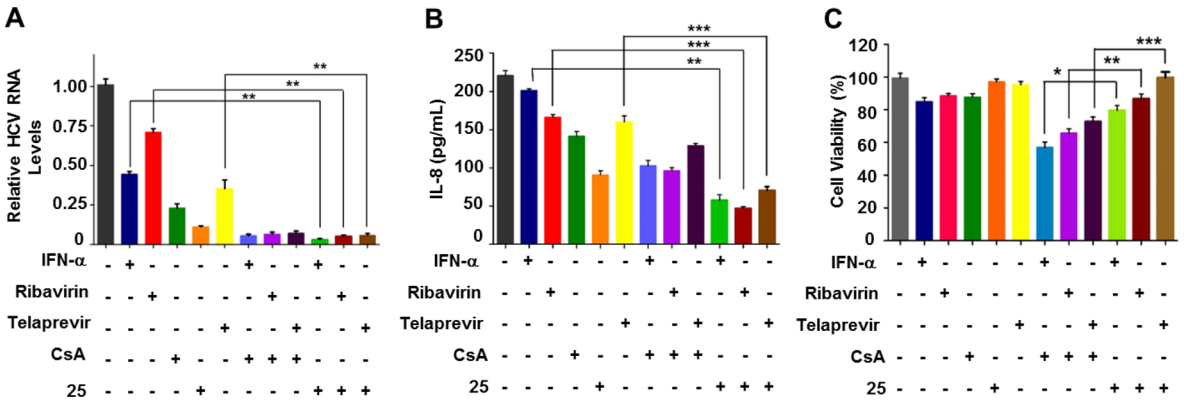

Figure 7. Combination treatment consisting of **25** and IFN-α, ribavirin, or telaprevir enhances the antiviral effect. (A) Real-time qRT-PCR analysis for HCV replicon RNA levels: (**) $P < 0.001$ vs the cells treated with IFN-α, ribavirin, or telaprevir. (B) ELISA analysis of the IL-8 levels: (**) $P < 0.01$ vs the cells treated with IFN-α; (***) $P < 0.001$ vs the cells treated with ribavirin or telaprevir. (C) MTT assay: (*) $P < 0.05$ vs the cells treated with CsA combined with IFN-α, (**) $P < 0.01$ vs the cells treated with CsA combined with ribavirin, (***) $P < 0.001$ vs the cells treated with CsA combined with telaprevir.

2-(4-Chlorophenyl)-*N*-cyclohexyl-2-[(2-1*H*-indol-3-ylacetyl)-phenylamino]acetamide (6). The procedures applied to the synthesis of **5** were used with cyclohexyl isocyanide **1a** (78 mg, 0.71 mmol), 4-chlorobenzaldehyde **2b** (100 mg, 0.71 mmol), aniline **3b** (83 mg, 0.89 mmol), 3-indoleacetic acid **4b** (187 mg, 1.06 mmol), and 2,2,2-trifluoroethanol at rt to obtain bis-amide **6** as a light yellow solid (97 mg, 27%) after extraction and purification by column chromatography (*n*-hexane/EtOAc = 3:1). Mp: 203.9−205.8 °C. IR (cm^{-1}): 3267, 1623. ^{1}H NMR (300 MHz, $CDCl_3$) δ: 7.97 (s, 1H), 7.40−7.30 (m, 5H), 7.22−7.02 (m, 8H), 6.92 (d, J = 2.4 Hz, 1H), 6.04 (s, 1H), 5.79−5.73 (m, 1H), 3.77−3.75 (m, 1H), 3.58 (s, 2H), 1.87−1.76 (m, 2H), 1.65−1.54 (m, 3H), 1.33−1.19 (m, 2H), 1.09−0.95 (m, 3H). ^{13}C NMR (125 MHz, $CDCl_3$) δ: 172.1, 168.3, 139.9, 135.9, 134.2, 133.1, 131.7, 130.2, 128.9, 128.3, 127.1, 123.1, 121.9, 119.4, 118.8, 110.9, 109.164.3, 48.6, 32.6, 31.9, 25.3, 24.7, 24.6. MS (ESI): m/z 522 $(M + Na)^+$, 498 $(M - H)^-$. HRMS (ESI): m/z 522.1921 $(M + Na)^+$ (calcd for $C_{30}H_{30}ClN_3NaO_2$, 522.1924), 500.2103 $(M + H)^+$ (calcd for $C_{30}H_{31}ClN_3O_2$, 500.2105). HPLC: purity 99.2%.

***N*-Cyclohexyl-2-[(2-1*H*-indol-3-ylacetyl)-(4-methoxyphenyl)-amino]-2-(4-nitrophenyl)acetamide (7).** The procedures applied to the synthesis of **5** were used with cyclohexyl isocyanide **1a** (72 mg, 0.66 mmol), 4-nitrobenzaldehyde **2a** (100 mg, 0.66 mmol), 4-methoxyaniline **3c** (123 mg, 0.82 mmol), 3-indoleacetic acid **4b** (103 mg, 0.66 mmol), and 2,2,2-trifluoroethanol at rt to obtain bis-amide **7** as a light yellow solid (30 mg, 8%). Mp: 205.5−207.9 °C. IR (cm^{-1}): 3310, 1634. ^{1}H NMR (500 MHz, $CDCl_3$) 8.19 (s, 1H), 7.99 (d, J = 8.5 Hz, 2H), 7.41 (d, J = 7.5 Hz, 1H), 7.30 (d, J = 8.0 Hz, 3H), 7.15 (t, J = 7.7 Hz, 1H), 7.05 (t, J = 7.5 Hz, 1H), 6.83 (s, 1H), 6.75−6.64 (b, 4H), 6.19 (s, 1H), 6.09 (d, J = 8.0 Hz, 1H), 3.76−3.70 (m, 4H), 3.60 (s, 2H), 1.81−1.75 (m, 2H), 1.62−1.53 (m, 3H), 1.32−1.23 (m, 2H), 1.08−1.01 (m, 1H), 0.94−0.87 (m, 2H). ^{13}C NMR (125 MHz, $CDCl_3$) δ: 172.8, 167.8, 159.3, 147.4, 141.8, 135.9, 132.0, 131.2, 131.0, 127.0, 123.0, 122.0, 119.5, 118.8, 114.2, 111.0, 108.7, 63.9, 55.3, 48.6, 32.48, 32.45, 31.8, 25.2, 24.68, 24.62. MS (ESI): m/z 563 $(M + Na)^+$, 539 $(M - H)^-$. Anal. Calcd for $C_{31}H_{32}N_4O_5 \cdot 0.02CH_2Cl_2$: C, 68.69; H, 5.95; N, 10.33. Found: C, 68.44; H, 5.86; N, 10.58. HPLC: purity 99.6%.

***N*-Cyclohexyl-2-[(2-1*H*-indol-3-ylacetyl)phenylamino]-2-phenylacetamide (8).** The procedures applied to the synthesis of **5** were used with cyclohexyl isocyanide **1a** (51 mg, 0.47 mmol), benzaldehyde **2c** (50 mg, 0.47 mmol), aniline **3b** (53 mg, 0.57 mmol), 3-indoleacetic acid **4b** (165 mg, 0.94 mmol), and methanol to obtain bis-amide **8** as a white solid (163 mg, 74%) after extraction and purification by column chromatography (*n*-hexane/EtOAc = 5:1, 1:1). Mp: 189−192 °C. IR (cm^{-1}): 3319, 1644. ^{1}H NMR (300 MHz, $CDCl_3$) δ: 8.03 (bs, 1H), 7.36 (d, J = 8.1 Hz, 1H), 7.31 (d, J = 8.1 Hz, 2H), 7.25−7.12 (m, 9H), 7.06−6.99 (m, 3H), 6.06 (s, 1H), 5.68 (d, J = 8.7 Hz, 1H), 3.84−3.73 (m, 1H), 3.58 (s, 2H), 1.90−1.80 (m, 2H), 1.63−1.51 (m, 3H), 1.38−1.22 (m, 2H), 1.11−0.89 (m, 3H). ^{13}C NMR (125 MHz, $CDCl_3$) δ: 172.0, 168.7, 140.2, 135.9, 134.7, 130.38, 130.3, 128.7, 128.2, 128.0, 127.2, 123.2, 121.7, 119.2, 118.8, 110.9, 109.2, 65.3, 48.6, 32.6, 31.8, 25.4, 24.7, 24.6. MS (ESI): m/z 488 $(M + Na)^+$, 464 $(M - H)^-$. HRMS (ESI): m/z 488.2314 $(M + Na)^+$ (calcd for $C_{30}H_{31}N_3NaO_2$, 488.2314), 466.2493 $(M + H)^+$ (calcd for $C_{30}H_{32}N_3O_2$, 466.2495). HPLC: purity 97.0%.

***N*-Cyclohexyl-2-[(2-1*H*-indol-3-ylacetyl)-(2-methoxyphenyl)-amino]-2-(3,4,5-trimethoxyphenyl)acetamide (9).** A mixture of 3,4,5-trimethoxybenzaldehyde **2d** (100 mg, 0.51 mmol) and *o*-anisidine **3d** (77 mg, 0.63 mmol) in methanol was stirred at 55 °C for 22 h. To the mixture was added cyclohexyl isocyanide **1a** (56 mg, 0.51 mmol) and 3-indoleacetic acid **4b** (110 mg, 0.63 mmol). The resulting reaction mixture was further heated at 55 °C for 45 h. The mixture was evaporated to dryness, washed with saturated $NaHCO_3$ solution, and extracted with EtOAc. The organic phase was dried over anhydrous sodium sulfate and was concentrated under reduced pressure. The residue was purified by column chromatography (*n*-hexane/EtOAc = 3:1, 1:1, EtOAc, MeOH) to obtain bis-amide **9** as a yellow solid (24 mg, 8%). Mp: 187.6−190.3 °C. IR (cm^{-1}): 3343, 1630. ^{1}H NMR (300 MHz, $CDCl_3$) δ: 7.97 (s, 1H), 7.46−7.37 (m, 2H), 7.32−7.27 (m, 2H), 7.25−7.11 (m, 3H), 7.07−6.99 (m, 1H), 6.94 (d, J = 2.1 Hz, 1H), 6.35 (s, 2H), 6.01 (d, J = 8.1 Hz, 1H), 5.94 (s, 1H), 3.81−3.72 (m, 1H), 3.73 (s, 3H), 3.61−3.56 (m, 9H), 3.39 (s, 2H), 1.95−1.79 (m, 2H), 1.65−1.48 (m, 3H), 1.32−1.23 (m, 2H), 1.19−0.94 (m, 3H). ^{13}C NMR (125 MHz, $CDCl_3$) δ: 172.5, 168.8, 155.6, 152.5, 152.0, 135.9, 132.0, 131.4, 129.4, 128.8, 127.3, 123.1, 121.8, 121.0, 120.5, 119.3, 118.9, 111.2, 110.9, 109.3, 107.9, 64.5, 60.6, 55.8, 54.9, 48.7, 32.7, 32.6, 31.5, 25.4, 24.7. MS (ESI): m/z 608 $(M + Na)^+$, 584 $(M - H)^-$. HRMS (ESI): m/z 608.2736 $(M + Na)^+$ (calcd for $C_{34}H_{39}N_3NaO_6$, 608.2737), 586.2916 $(M + H)^+$ (calcd for $C_{34}H_{40}N_3O_6$, 586.2917). HPLC: purity 99.7%.

***N*-Cyclohexyl-2-[(3,4-dimethoxyphenyl)-(2-1*H*-indol-3-ylacetyl)amino]-2-(2,3,4-trimethoxyphenyl)acetamide (10).** The procedures applied to the synthesis of **5** were used with cyclohexyl isocyanide **1a** (55 mg, 0.50 mmol), 2,3,4-trimethoxybenzaldehyde **2e** (100 mg, 0.51 mmol), 4-aminoveratrole **3e** (97 mg, 0.63 mmol), 3-indoleacetic acid **4b** (88 mg, 0.50 mmol), and 2,2,2-trifluoroethanol at rt to obtain bis-amide **10** as a light orange solid (253 mg, 80%) after extraction and purification by column chromatography (EtOAc). Mp: 113.8−115.8 °C. IR (cm^{-1}): 3356, 1647. ^{1}H NMR (300 MHz, $CDCl_3$) δ: 8.20 (s, 1H), 7.34−7.28 (m, 3H), 7.14−7.09 (m, 1H), 7.04−6.98 (m, 2H), 6.69−6.53 (m, 2H), 6.38 (s, 1H), 6.34 (d, J = 8.7 Hz, 1H), 5.93 (bs, 1H), 5.64 (d, J = 8.1 Hz, 1H), 3.83−3.76 (m, 15H), 3.60 (s, 2H), 3.36 (bs, 1H), 1.90−1.82 (m, 2H), 1.66−1.53 (m, 3H), 1.37−1.23 (m, 2H), 1.13−0.92 (m, 3H). ^{13}C NMR (125 MHz, $CDCl_3$) δ: 172.2, 169.3, 153.7, 152.2, 148.3, 141.2, 135.9, 132.9, 127.2, 125.8, 123.0, 121.7, 120.5, 119.2, 118.8,

DOI: 10.1021/acs.jmedchem.5b01064
J. Med. Chem. XXXX, XXX, XXX−XXX

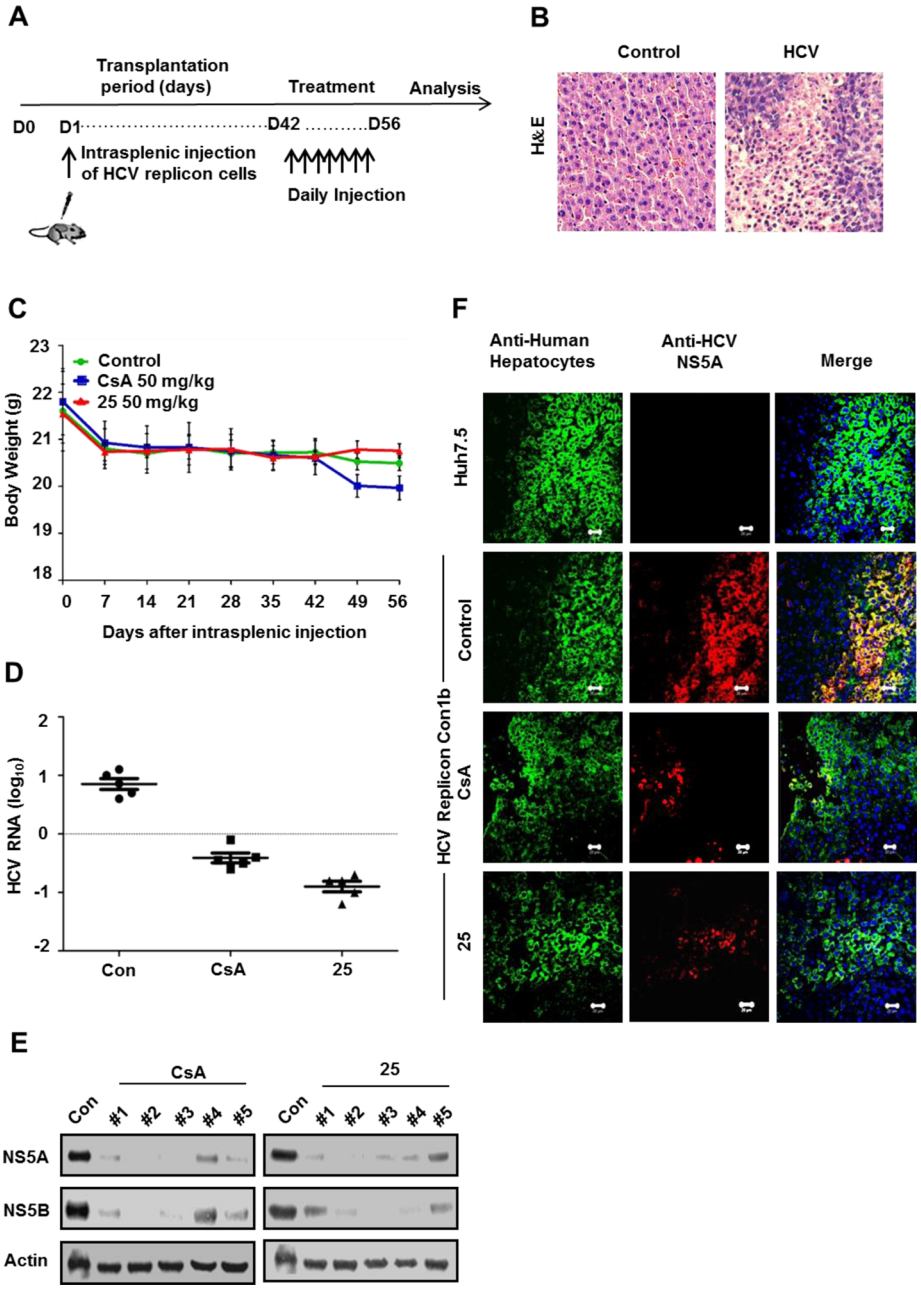

Figure 8. Lead **25** abolishes viral replication in an HCV mouse model. (A) Schematic representation of the in vivo experiments using NOD/SCID mice. (B) Hematoxylin and eosin staining: histological examination of control and HCV replicon cells transplanted in mouse liver tissue. (C) Body weight changes of the mice. (D) HCV RNA levels in the liver of the mice assessed by real time qRT-PCR analysis. (E) HCV NS5A expression level after treatment with CsA or **25**. (F) Confocal microscopy analysis of Huh7 cells or Huh7 cells containing the HCV-Con1b replicon for human hepatocytes (green) and HCV NS5A (red). The nuclei were stained with DAPI (blue). The colocalization of human hepatocytes with HCV NS5A is shown in yellow. All data are representative of three different experiments.

113.2, 110.8, 110.1, 109.6, 106.4, 61.0, 60.5, 58.3, 55.8, 55.7, 48.5, 32.7, 31.8, 25.4, 24.8, 24.7. MS (ESI): m/z 638 $(M + Na)^+$, 614 $(M - H)^-$. HRMS (ESI): m/z 638.2839 $(M + Na)^+$ (calcd for $C_{35}H_{41}N_3NaO_7$, 638.2842), 616.3014 $(M + H)^+$ (calcd for $C_{35}H_{42}N_3O_7$, 616.3023). HPLC: purity 99.9%.

***N*-(1-(4-Chlorophenyl)-2-(cyclohexylamino)-2-oxoethyl)-*N*-(4-isopropylphenyl)-3-(4-methoxyphenyl)propanamide (11).** The procedures applied to the synthesis of **5** were used with cyclohexyl isocyanide **1a** (77 mg, 0.71 mmol), 4-chlorobenzaldehyde **2b** (100 mg, 0.71 mmol), 4-isopropylaniline **3f** (120 mg, 0.89 mmol), 3-(4-methoxyphenyl)propionic acid **4a** (193 mg, 1.07 mmol), and 2,2,2-trifluoroethanol at rt to obtain bis-amide **11** as a white solid (120 mg, 30%). Mp: 205.1−207.8 °C. IR (cm^{-1}): 3258, 1643. ^1H NMR (300 MHz, $CDCl_3$) δ: 7.15−7.12 (m, 2H), 7.05−7.02 (m, 6H), 6.96−6.94 (m, 2H), 6.76−6.74 (m, 2H), 5.89 (s, 1H), 5.80−5.77 (m, 1H), 3.80−3.72 (m, 1H), 3.75 (s, 3H), 2.87−2.82 (m, 3H), 2.36−2.30 (m, 2H), 1.93−1.80 (m, 2H), 1.67−1.55 (m, 3H), 1.38−1.26 (m, 2H), 1.20−1.00 (m, 3H), 1.18 (d, J = 6.9 Hz, 6H). ^{13}C NMR (125 MHz, $CDCl_3$) δ: 173.1, 168.3, 157.8, 149.1, 137.4, 134.1, 133.3, 133.1, 131.5, 129.7, 129.3, 128.2, 127.0, 113.6, 64.6, 55.2, 48.6, 36.8, 33.6, 32.8, 32.7, 30.5, 25.4, 24.7, 23.9, 23.8. MS (ESI): m/z 569 $(M + Na)^+$. HRMS (ESI): m/z 569.2549 $(M + Na)^+$ (calcd for $C_{33}H_{39}ClN_2NaO_3$, 569.2547), 547.2729 $(M + H)^+$ (calcd for $C_{33}H_{40}ClN_2O_3$, 547.2727). HPLC: purity 97.1%.

***N*-Cyclohexyl-2-(3,4-dimethoxyphenyl)-2-[(2-1*H*-indol-3-ylacetyl)phenylamino]acetamide (12).** The procedures applied to

DOI: 10.1021/acs.jmedchem.5b01064
J. Med. Chem. XXXX, XXX, XXX−XXX

the synthesis of **9** were used with cyclohexyl isocyanide **1a** (65 mg, 0.60 mmol), 3,4-dimethoxybenzaldehyde **2f** (100 mg, 0.60 mmol), aniline **3b** (70 mg, 0.75 mmol), 3-indoleacetic acid **4b** (126 mg, 0.72 mmol), and methanol to obtain bis-amide **12** as a white solid (86 mg, 27%). Mp: 183.0−187.9 °C. IR (cm^{-1}): 3293, 1661. ^1H NMR (300 MHz, $CDCl_3$) δ: 8.06 (s, 1H), 7.39 (d, J = 7.8 Hz, 1H), 7.30 (d, J = 8.1 Hz, 1H), 7.19−7.11 (m, 5H), 7.06−6.97 (m, 2H), 6.77−6.64 (m, 3H), 6.52 (s, 1H), 6.07 (s, 1H), 5.69 (d, J = 8.1 Hz, 1H), 3.81 (s, 3H), 3.79−3.73 (m, 1H), 3.58 (s, 2H), 3.53 (s, 3H), 1.89−1.79 (m, 2H), 1.63−1.53 (m, 3H), 1.34−1.23 (m, 2H), 1.13−0.91 (m, 3H). ^{13}C NMR (150 MHz, $CDCl_3$) δ: 171.9, 168.9, 148.8, 148.2, 140.0, 135.9, 130.5, 128.7, 128.0, 127.2, 126.9, 123.2, 123.2, 121.7, 119.2, 118.8, 113.2, 110.9, 110.3, 109.2, 64.3, 55.6, 55.5, 48.6, 32.7, 32.6, 31.8, 25.4, 24.7, 24.6. MS (ESI): m/z 548 $(M + Na)^+$, 524 $(M - H)^-$. Anal. Calcd for $C_{32}H_{35}N_3O_4 \cdot 0.05CH_2Cl_2$: C, 72.66; H, 6.68; N, 7.93. Found: C, 72.68; H, 6.68; N, 8.20. HPLC: purity 99.9%.

***N*-(1-(Benzo[*d*][1,3]dioxol-5-yl)-2-oxo-2-(pentylamino)-ethyl)-*N*-(3,4-dimethoxyphenyl)pentanamide (13).** The procedures applied to the synthesis of **5** were used with 1-pentyl isocyanide **1b** (65 mg, 0.67 mol), piperonal **2g** (100 mg, 0.67 mmol), 4-aminoveratrole **3e** (128 mg, 0.83 mmol), valeric acid **4c** (85 mg, 0.83 mmol), and methanol at rt to obtain bis-amide **13** as a yellow solid (178 mg, 55%) after purification by column chromatography (*n*-hexane/EtOAc = 1:1). Mp: 98.9−100.8 °C. IR (cm^{-1}): 3278, 1651. ^1H NMR (300 MHz, $CDCl_3$) δ: 6.83−6.50 (m, 5H), 6.32−6.01 (m, 2H), 5.89 (s, 2H), 5.76 (bs, 1H), 3.84 (s, 4H), 3.71 (bs, 2H), 3.26 (q, J = 7.2 Hz, 2H), 2.09−2.03 (m, 2H), 1.59−1.51 (m, 2H), 1.49−1.42 (m, 2H), 1.30−1.18 (m, 6H), 0.88−0.78 (m, 6H). ^{13}C NMR (150 MHz, $CDCl_3$) δ: 174.1, 169.8, 148.6, 148.4, 147.5, 132.8, 128.5, 124.2, 122.7, 113.4, 110.3, 107.9, 101.1, 64.6, 55.9, 55.8, 39.8, 34.3, 29.1, 28.9, 27.5, 22.3, 22.2, 13.9, 13.8. MS (ESI): m/z 507 $(M + Na)^+$. Anal. Calcd for $C_{27}H_{36}N_2O_6$: C, 66.92; H, 7.49; N, 5.78. Found: C, 66.88; H, 7.42; N, 5.92. HPLC: purity 95.0%.

***N*-Cyclohexyl-2-[(2-1*H*-indol-3-ylacetyl)phenylamino]-2-(3,4,5-trimethoxyphenyl)acetamide (14).** The procedures applied to the synthesis of **9** were used with cyclohexyl isocyanide **1a** (38 mg, 0.35 mmol), 3,4,5-trimethoxybenzaldehyde **2d** (70 mg, 0.35 mmol), aniline **3b** (41 mg, 0.44 mmol), 3-indoleacetic acid **4b** (130 mg, 0.74 mmol), and methanol to obtain bis-amide **14** as a beige ash (118 mg, 59%) after extraction and purification by MPLC (*n*-hexane/EtOAc = 3:1, 1:1 and EtOAc). Mp: 156−158 °C. IR (cm^{-1}): 3261, 1650. ^1H NMR (300 MHz, $CDCl_3$) δ: 8.00 (s, 1H), 7.41 (d, J = 7.8 Hz, 2H), 7.31 (d, J = 8.1 Hz, 2H), 7.24−7.19 (m, 2H), 7.14 (t, J = 7.2 Hz, 2H), 7.04 (t, J = 7.2 Hz, 1H), 6.95 (s, 1H), 6.30 (s, 2H), 6.07 (s, 1H), 5.75 (d, J = 7.8 Hz, 1H), 3.83−3.71 (m, 1H), 3.76 (s, 3H), 3.60 (s, 2H), 3.58 (s, 6H), 1.89−1.80 (m, 2H), 1.68−1.56 (m, 3H), 1.38−1.23 (m, 2H), 1.14−0.92 (m, 3H). ^{13}C NMR (125 MHz, $CDCl_3$) δ: 171.9, 168.6, 152.6, 140.0, 137.8, 135.9, 130.5, 129.8, 128.7, 128.1, 127.2, 123.1, 121.8, 119.3, 118.9, 110.9, 109.2, 107.6, 64.5, 60.7, 55.9, 48.6, 32.7, 31.9, 25.4, 24.8, 24.7. MS (ESI): m/z 578 $(M + Na)^+$, 554 $(M - H)^-$. HRMS (ESI): m/z 578.2629 $(M + Na)^+$ (calcd for $C_{33}H_{37}N_3NaO_5$, 578.2631), 556.2809 $(M + H)^+$ (calcd for $C_{33}H_{38}N_3O_5$, 556.2811). HPLC: purity 99.5%.

***N*-[Cyclohexylcarbamoyl-(4-hydroxyphenyl)methyl]-*N*-(3,4-dimethoxyphenyl)-3-(3-methoxyphenyl)propionamide (15).** A mixture of 4-hydroxybenzaldehyde **2h** (500 mg, 4.15 mmol) and 4-aminoveratrole **3e** (950 mg, 6.23 mmol) in methanol was stirred at rt. The solid thus formed was filtered off to obtain imine. The imine (150 mg, 0.60 mmol) was added to the mixture of cyclohexyl isocyanide **1a** (80 mg, 0.73 mmol) and 3-(3-methoxyphenyl)propionic acid **4d** (170 mg, 0.90 mmol) in methanol, and the resulting reaction mixture was stirred at rt to obtain bis-amide **15** as a white solid (116 mg, 36%) after filtration. Mp: 187.5−189.1 °C. IR (cm^{-1}): 3283, 1660. ^1H NMR (300 MHz, $CDCl_3$) δ: 7.12 (t, J = 8.1 Hz, 1H), 6.93 (d, J = 8.1 Hz, 2H), 6.70−6.59 (m, 4H), 6.46 (bs, 1H), 6.16 (bs, 1H), 5.95 (bs, 2H), 5.85 (bs, 1H), 5.64−5.62 (m, 1H), 3.79 (bs, 6H), 3.74 (s, 3H), 3.50−3.42 (m, 1H), 2.89 (t, J = 7.8 Hz, 2H), 2.42−2.33 (m, 2H), 1.94−1.80 (m, 2H), 1.59−1.56 (m, 3H), 1.35−1.26 (m, 2H), 1.16−0.95 (m, 3H). ^{13}C NMR (125 MHz, $CDCl_3$) δ: 173.2, 159.4, 156.3, 148.4, 142.7, 132.5, 131.8, 129.2, 126.2, 122.7, 120.7, 115.2, 114.1, 113.4, 111.2, 110.4, 64.4, 55.7, 55.0, 48.7, 36.4, 32.7, 31.6, 25.4, 24.7, 24.6. MS (ESI): m/z 569 $(M + Na)^+$. HRMS (ESI): m/z 569.2626 $(M + Na)^+$ (calcd for $C_{32}H_{38}N_2NaO_6$, 569.2628), 547.2808 $(M + H)^+$ (calcd for $C_{32}H_{39}N_2O_6$, 547.2808). HPLC: purity 99.7%.

***N*-(1-(4-Chlorophenyl)-2-(cyclohexylamino)-2-oxoethyl)-*N*-(3,4-dimethoxyphenyl)-3-(4-methoxyphenyl)propanamide (16).** The procedures applied to the synthesis of **5** were used with cyclohexyl isocyanide **1a** (77 mg, 0.71 mmol), 4-chlorobenzaldehyde **2b** (100 mg, 0.7 mmol), 4-aminoveratrole **3e** (128 mg, 0.91 mmol), 3-(4-methoxyphenyl)propionic acid **4a** (200 mg, 1.10 mmol), and methanol at rt to obtain bis-amide **16** as a white solid (55 mg, 14%) after purification by column chromatography (*n*-hexane/EtOAc = 1:1). Mp: 195.6−197.3 °C. IR (cm^{-1}): 3286, 1650. ^1H NMR (300 MHz, $CDCl_3$) δ: 7.15 (d, J = 8.1 Hz, 2H), 7.04 (d, J = 8.1 Hz, 2H), 6.98 (d, J = 8.7 Hz, 3H), 6.96 (d, J = 8.7 Hz, 3H), 6.50 (bs, 1H), 5.99 (s, 1H), 5.65 (bs, 1H), 3.82 (s, 6H), 3.76 (s, 3H), 3.51−3.46 (m, 1H), 2.86 (t, J = 7.5 Hz, 2H), 2.38−2.31 (m, 2H), 1.96−1.81 (m, 2H), 1.71−1.62 (m, 3H), 1.41−1.26 (m, 2H), 1.18−1.05 (m, 3H). ^{13}C NMR (125 MHz, $CDCl_3$) δ: 173.3,157.8, 148.6, 134.3, 133.1, 132.2, 131.8, 129.3, 128.4, 122.7, 113.7, 113.3, 110.5, 63.9, 55.8, 55.7, 55.2, 55.1, 48.7, 36.5, 32.8, 30.6, 25.4, 24.8, 24.7. MS (ESI): m/z 587 $(M + Na)^+$, 563 $(M - H)^-$. HRMS (ESI): m/z 587.2287 $(M + Na)^+$ (calcd for $C_{32}H_{37}ClN_2NaO_5$, 587.2289), 565.2470 $(M + H)^+$ (calcd for $C_{32}H_{38}ClN_2O_5$, 565.2469). HPLC: purity 99.6%.

***N*-[Cyclohexylcarbamoyl-(4-nitrophenyl)methyl]-*N*-[2-(3,4-dimethoxyphenyl)ethyl]-5-methoxy-2-nitrobenzamide (17).** The procedures applied to the synthesis of **15** were used with cyclohexyl isocyanide **1a** (35 mg, 0.32 mmol), imine formed by reaction of 4-nitrobenzaldehyde **2a**, and 3,4-dimethoxyphenethylamine **3g** in methanol (100 mg, 0.32 mmol), 5-methoxy-2-nitrobenzoic acid **4e** (79 mg, 0.40 mmol), and methanol at rt to obtain bis-amide **17** as a yellow solid (196 mg, 99%) after purification by column chromatography (*n*-hexane/EtOAc = 3:1). Mp: 104.5−107.6 °C. IR (cm^{-1}): 3327, 1642. ^1H NMR (300 MHz, $CDCl_3$) δ: 8.31−8.22 (m, 3H), 7.78 (bs, 2H), 7.02 (dd, J = 9.3, 2.7 Hz, 1H), 6.77−6.62 (m, 3H), 6.24 (d, J = 7.8 Hz, 1H), 6.14 (s, 1H), 5.94−5.83 (m, 1H), 3.97−3.91 (m, 1H), 3.92 (s, 3H), 3.79 (s, 3H), 3.69 (s, 3H), 3.38−3.32 (m, 2H), 2.70−2.57 (m, 2H), 2.04−1.98 (m, 2H), 1.75−1.64 (m, 3H), 1.41−1.32 (m, 2H), 1.28−1.19 (m, 3H). ^{13}C NMR (150 MHz, $CDCl_3$) δ: 168.3, 166.5, 164.3, 148.9, 147.8, 137.5, 130.5, 129.8, 129.5, 127.5, 123.8, 120.2, 114.5, 114.3, 113.9, 113.6, 111.2, 111.1, 63.4, 62.6, 56.3, 55.8, 55.6, 51.2, 50.8, 49.0, 34.9, 32.7, 32.6, 25.3, 24.7. MS (ESI): m/z 643 $(M + Na)^+$, 619 $(M - H)^-$. HRMS (ESI): m/z 643.2373 $(M + Na)^+$ (calcd for $C_{32}H_{36}N_4NaO_9$, 643.2380), 621.2551 $(M + H)^+$ (calcd for $C_{32}H_{37}N_4O_9$, 621.2561). HPLC: purity 99.3%.

***N*-Cyclohexyl-2-(4-fluorophenyl)-2-[(2-1*H*-indol-3-ylacetyl)-(4-methoxyphenyl)amino]acetamide (18).** The procedures applied to the synthesis of **5** were used with cyclohexyl isocyanide **1a** (87 mg, 0.80 mmol), 4-fluorobenzaldehyde **2i** (100 mg, 0.80 mmol), 4-methoxyaniline **3c** (124 mg, 1.00 mmol), 3-indoleacetic acid **4b** (176 mg, 1.00 mmol), and methanol at rt to obtain bis-amide **18** as a white solid (290 mg, 70%). Mp: 209.3-213.8 °C. IR (cm^{-1}): 3267, 1657. ^1H NMR (300 MHz, $CDCl_3$) δ: 8.05 (s, 1H), 7.39 (d, J = 6.9 Hz, 2H), 7.33−7.30 (m, 1H), 7.17−7.01 (m, 4H), 6.97 (d, J = 2.1 Hz, 1H), 6.87−6.81 (m, 2H), 6.77−6.56 (m, 2H), 6.43−6.27 (m, 1H), 6.12 (s, 1H), 5.76 (d, J = 8.4 Hz, 1H), 3.79−3.69 (m, 1H), 3.75 (s, 3H), 3.57 (s, 2H), 1.87−1.77 (m, 2H), 1.64−1.53 (m, 3H), 1.35−1.23 (m, 2H), 1.11−0.88 (m, 3H). ^{13}C NMR (150 MHz, $CDCl_3$) δ: 172.5, 168.6, 163.2, 161.6, 159.0, 135.9, 132.3, 132.2, 131.4, 130.5,3 130.5, 127.2, 123.1, 121.8, 119.3, 118.9, 115.1, 115.0, 113.8, 110.9, 109.2, 63.7, 55.3, 48.5, 32.6, 31.8, 25.3, 24.7, 24.6. MS (ESI): m/z 536 $(M + Na)^+$, 514 $(M + H)^+$. Anal. Calcd for $C_{31}H_{32}FN_3O_3$: C, 72.49; H, 6.28; N, 8.18. Found: C, 72.26; H, 6.12; N, 8.48. HPLC: purity 96.9%.

***N*-[Cyclohexylcarbamoyl(4-hydroxyphenyl)methyl]-*N*-(3,4-dimethoxyphenyl)-2,3-dimethylbenzamide (19).** The procedures applied to the synthesis of **15** were used with cyclohexyl isocyanide **1a** (66 mg, 0.60 mmol), imine formed by the reaction of 4-hydroxybenzaldehyde **2h** and 4-aminoveratrole **3e** in methanol (150 mg, 0.60 mmol), 2,3-dimethylbenzoic acid **4f** (135 mg, 0.90 mmol), and methanol at rt to obtain bis-amide **19** as a white solid (170 mg,

DOI: 10.1021/acs.jmedchem.5b01064
J. Med. Chem. XXXX, XXX, XXX−XXX

56%). Mp: 157.2−161.2 °C. ^{1}H NMR (300 MHz, $CDCl_3$) δ: 7.05 (d, J = 8.1 Hz, 2H), 6.89−6.80 (m, 2H), 6.06 (d, J = 8.1 Hz, 2H), 6.56−6.46 (m, 2H), 6.39−6.35 (m, 2H), 6.18 (s, 1H), 5.69 (d, J = 8.4 Hz, 1H), 3.91−3.81 (m, 1H), 3.68 (s, 3H), 3.58 (s, 3H), 2.28 (s, 3H), 2.11 (s, 3H), 1.97−1.87 (m, 2H), 1.66−1.56 (m, 3H), 1.42−1.29 (m, 2H), 1.18−1.04 (m, 3H). ^{13}C NMR (75 MHz, DMSO-d_6) δ: 171.4, 169.8, 157.2, 147.6, 147.4, 138.7, 136.9, 133.0, 132.0, 129.6, 126.2, 125.1, 125.0, 123.9, 115.3, 110.2, 63.9, 55.8, 55.6, 48.6, 32.9, 32.8, 25.9, 25.3, 25.2, 20.2, 17.2. MS (ESI): m/z 539 (M + Na)$^+$. HRMS (ESI): m/z 539.2526 (M + Na)$^+$ (calcd for $C_{31}H_{36}N_2NaO_5$, 539.2522), 517.2706 (M + H)$^+$ (calcd for $C_{31}H_{37}N_2O_5$, 517.2702). HPLC: purity 98.9%.

***N*-(1-(4-Chlorophenyl)-2-(cyclohexylamino)-2-oxoethyl)-*N*-(4-isopropylphenyl)benzamide (20).** The procedures applied for synthesis of **5** was used with cyclohexyl isocyanide **1a** (77 mg, 0.71 mmol), 4-chlorobenzaldehyde **2b** (100 mg, 0.71 mmol), 4-isopropylaniline **3f** (120 mg, 0.89 mmol), benzoic acid **4g** (131 mg, 1.07 mmol), and 2,2,2-trifluoroethanol at rt to obtain bis-amide **20** as a white solid (82 mg, 23%). Mp: 181.0−182.5 °C. IR (cm^{-1}): 3276, 1658. ^{1}H NMR (300 MHz, $CDCl_3$) δ: 7.31−7.28 (m, 2H), 7.23 (d, J = 1.5 Hz, 4H), 7.20−7.09 (m, 3H), 6.91−6.84 (m, 5H), 6.05 (s, 1H), 5.99 (d, J = 8.1 Hz, 1H), 3.91−3.82 (m, 1H), 2.74 (heptet, J = 6.9 Hz, 1H), 1.98−1.88 (m, 2H), 1.68−1.58 (m, 3H), 1.44−1.29 (m, 2H), 1.24−1.19 (m, 3H), 1.10 (d, J = 6.9 Hz, 6H). ^{13}C NMR (125 MHz, $CDCl_3$) δ: 171.2, 168.2, 148.2, 138.9, 135.7, 134.2, 133.5, 131.3, 129.6, 128.57, 128.53, 127.5, 126.5, 66.4, 48.6, 33.4, 32.8, 25.4, 24.7, 24.6, 23.77, 23.74. MS (ESI) m/z = 511 (M + Na)$^+$. HPLC: purity 99.2%.

2-[Acetyl-(4-isopropylphenyl)amino]-2-(4-chlorophenyl)-*N*-cyclohexylacetamide (21). The procedures applied to the synthesis of **15** were used with cyclohexyl isocyanide **1a** (55 mg, 0.48 mmol), the imine formed by the reaction of 4-chlorobenzaldehyde **2b** and 4-isopropylaniline **3f** in methanol (100 mg, 0.38 mmol), acetic acid **4h** (35 mg, 0.57 mmol), and methanol at rt to obtain bis-amide **21** as a white solid (40 mg, 24%) after filtration. Mp: 184.7−186.0 °C. IR (cm^{-1}): 3272, 1658. ^{1}H NMR (300 MHz, $CDCl_3$) δ: 7.17−7.13 (m, 2H), 7.10−7.05 (m, 4H), 6.96 (bs, 2H), 5.93 (s, 1H), 5.74 (d, J = 8.1 Hz, 1H), 3.85−3.75 (m, 1H), 2.85 (heptet, J = 6.9 Hz, 1H), 2.17−1.83 (m, 2H), 1.86 (s, 3H), 1.70−1.56 (m, 3H), 1.41−1.27 (m, 2H), 1.19 (d, J = 6.9 Hz, 6H), 1.18−1.07 (m, 3H). ^{13}C NMR (125 MHz, $CDCl_3$) δ: 171.5, 168.4, 149.1, 138.1, 134.3, 133.3, 131.6, 129.7, 128.3, 127.0, 64.4, 48.7, 33.6, 32.8, 32.7, 25.4, 24.78, 24.71, 23.9, 23.8, 23.2. MS (ESI): m/z 449 (M + Na)$^+$. Anal. Calcd for $C_{25}H_{31}ClN_2O_2\cdot 0.25H_2O$: C, 69.59; H, 7.36; N, 6.49. Found: C, 69.56; H, 7.26; N, 6.58. HPLC: purity 98.7%.

***N*-[Cyclohexylcarbamoyl-(4-nitrophenyl)methyl]-*N*-(3,4-dimethoxyphenyl)-2,5-dimethylbenzamide (22).** The procedures applied to the synthesis of **15** were used with cyclohexyl isocyanide **1a** (47 mg, 0.35 mmol), the imine formed by the reaction of 4-nitrobenzaldehyde **2a** and 4-aminoveratrole **3e** in 2,2,2-trifluoroethanol (100 mg, 0.35 mmol), 2,5-dimethylbenzoic acid **4i** (66 mg, 0.44 mmol), and methanol at rt to obtain bis-amide **22** as a dark green solid (48 mg, 25%) after purification by column chromatography (*n*-hexane/EtOAc = 3:1). Mp: 175.9−177.9 °C. IR (cm^{-1}): 3346, 1630. ^{1}H NMR (600 MHz, $CDCl_3$) δ: 8.10 (d, J = 8.4 Hz, 2H), 7.49 (d, J = 8.4 Hz, 2H), 6.88−6.85 (m, 3H), 6.63 (s, 1H), 6.46−6.40 (m, 2H), 6.29 (s, 1H), 6.07 (s, 1H), 3.92−3.86 (m, 1H), 3.70 (s, 3H), 3.61 (s, 3H), 2.31 (s, 3H), 2.14 (s, 3H), 2.02 (d, J = 10.8 Hz, 1H), 1.93 (d, J = 8.4 Hz, 1H) 1.74−1.60 (m, 3H), 1.44−1.34 (m, 2H), 1.23−1.10 (m, 3H). ^{13}C NMR (150 MHz, $CDCl_3$) δ: 172.6, 167.7, 148.2, 148.1, 147.6, 141.9, 135.7, 134.3, 133.4, 131.7, 131.1, 129.9, 129.5, 127.4, 123.4, 122.0, 113.2, 109.8, 55.8, 55.6, 48.9, 32.8, 25.4, 24.7, 24.6, 20.7, 18.9. MS (ESI): m/z 544 (M − H)$^-$. Anal. Calcd for $C_{31}H_{35}N_3O_6\cdot 1.05CH_4O\cdot 0.4H_2O$: C, 65.64; H, 6.87; N, 7.16. Found: C, 65.39; H, 6.62; N, 6.90. HPLC: purity 98.0%.

***N*-[Cyclohexylcarbamoyl-(4-nitrophenyl)methyl]-*N*-[2-(3,4-dimethoxyphenyl)ethyl]benzamide (23).** The procedures applied to the synthesis of **15** were used with cyclohexyl isocyanide **1a** (35 mg, 0.32 mmol), the imine formed by the reaction of 4-nitrobenzaldehyde **2a** and 3,4-dimethoxyphenethylamine **3g** in methanol (100 mg, 0.32 mmol), benzoic acid **4g** (49 mg, 0.44 mmol), and methanol at rt to obtain bis-amide **23** as a white solid (112 mg, 64%) after filtration. Mp: 194.3−198.0 °C. IR (cm^{-1}): 3266, 1675. ^{1}H NMR (500 MHz, $CDCl_3$) δ: 8.25 (d, J = 8.5 Hz, 2H), 7.68 (bs, 2H), 7.50−7.43 (m, 5H), 6.75−6.26 (m, 2H), 6.25 (bs, 1H), 6.06−5.97 (m, 2H), 3.92−3.85 (m, 1H), 3.79 (s, 3H), 3.68 (s, 3H), 3.55 (bs, 2H), 2.67 (bs, 1H), 2.38−2.32 (m, 1H), 1.98−1.92 (m, 2H), 1.74−1.69 (m, 2H), 1.64−1.60 (m, 1H), 1.44−1.35 (m, 2H), 1.22−1.14 (m, 3H). ^{13}C NMR (125 MHz, $CDCl_3$) δ: 148.8, 147.7, 147.6, 142.8, 135.7, 130.1, 129.4, 128.7, 126.6, 123.8, 120.5, 111.5, 111.1, 55.8, 55.7, 48.7, 32.78, 32.72, 25.4, 24.6. MS (ESI): m/z 568 (M + Na)$^+$. Anal. Calcd for $C_{31}H_{35}N_3O_6\cdot 0.7H_2O$: C, 66.7; H, 6.57; N, 7.53. Found: C, 66.62; H, 6.51; N, 7.63. HPLC: purity 95.0%.

6-Chloro-*N*-[cyclohexylcarbamoyl-(4-nitrophenyl)methyl]-*N*-[2-(3-methoxyphenyl)ethyl]nicotinamide (24). The procedures applied to the synthesis of **5** were used with cyclohexyl isocyanide **1a** (72 mg, 0.66 mmol), 4-nitrobenzaldehyde **2a** (100 mg, 0.66 mmol), 2-(3-methoxyphenyl)ethylamine **3h** (125 mg, 0.83 mmol), 6-chloronicotinic acid **4j** (131 mg, 0.83 mmol), and methanol at rt to obtain bis-amide **24** as a yellow solid (296 mg, 81%). Mp: 87.5−90.8 °C. IR (cm^{-1}): 3286, 1636. ^{1}H NMR (500 MHz, $CDCl_3$) δ: 8.40 (s, 1H), 8.26 (d, J = 8.5 Hz, 2H), 7.68−7.58 (m, 3H), 7.37 (d, J = 8.5 Hz, 1H), 7.08 (t, J = 7.7 Hz, 1H), 6.71−6.68 (m, 1H), 6.33−6.20 (m, 3H), 5.86 (bs, 1H), 3.90−3.82 (m, 1H), 3.69 (s, 3H), 3.61 (bs, 2H), 2.61 (bs, 1H), 2.39 (bs, 1H), 1.97−1.91 (m, 2H), 1.72−1.67 (m, 2H), 1.64−1.59 (m, 1H), 1.43−1.33 (m, 2H), 1.22−1.10 (m, 3H). ^{13}C NMR (125 MHz, $CDCl_3$) δ: 159.7, 152.8, 147.9, 147.4, 137.2, 130.4, 129.9, 129.6, 124.3, 124.1, 120.8, 114.2, 112.0, 55.0, 49.0, 32.75, 32.72, 25.3, 24.68, 24.66. MS (ESI): m/z 549 (M − H)$^-$. Anal. Calcd for $C_{29}H_{31}ClN_4O_5\cdot 0.6H_2O$: C, 61.99; H, 5.78; N, 9.97. Found: C, 61.91; H, 5.78; N, 10.07. HPLC: purity 99.4%.

***N*-Cyclohexyl-2-[(2-1*H*-indol-3-ylacetyl)-(4-isopropylphenyl)-amino]-2-(3,4,5-trimethoxyphenyl)acetamide (25).** The procedures applied to the synthesis of **15** were used with cyclohexyl isocyanide **1a** (69 mg, 0.63 mmol), crude mixture containing imine formed by the reaction of 3,4,5-trimethoxybenzaldehyde **2d** and 4-isopropylaniline **3f** in ethanol under reflux condition (200 mg, ∼0.63 mmol), 3-indoleacetic acid **4b** (235 mg, 1.34 mmol), and methanol at 55 °C to obtain bis-amide **25** as an ivory solid (260 mg, 69%) after purification by column chromatography (*n*-hexane/EtOAc = 3:1, 1:1). Mp: 141−143 °C. IR (cm^{-1}): 3315, 1644. ^{1}H NMR (600 MHz, $CDCl_3$) δ: 8.29 (s, 1H), 7.37 (d, J = 7.8 Hz, 1H), 7.30 (d, J = 7.8 Hz, 1H), 7.14−6.94 (m, 4H, overlapped), 7.12 (t, J = 7.8 Hz, 1H, overlapped), 7.02 (t, J = 7.8 Hz, 1H, overlapped), 6.94 (d, J = 1.8 Hz, 1H, overlapped), 6.29 (s, 2H), 6.09 (s, 1H), 5.81 (d, J = 8.4 Hz, 1H), 3.80−3.74 (m, 1H, overlapped), 3.76 (s, 3H, overlapped), 3.60 (d, J = 2.4 Hz, 2H), 3.58 (s, 6H), 2.84 (heptet, J = 6.9 Hz, 1H), 1.83 (dd, J = 33.0, 9.6 Hz, 2H), 1.64−1.54 (m, 3H), 1.34−1.25 (m, 2H), 1.19 (d, J = 7.2 Hz, 6H), 1.10−0.95 (m, 3H). ^{13}C NMR (150 MHz, $CDCl_3$) δ: 172.2, 168.6, 152.6, 149.0, 137.6, 137.4, 135.9, 130.2, 129.9, 127.2, 126.7, 123.1, 121.8, 119.3, 118.9, 110.9, 109.3, 107.7, 64.3, 60.7, 55.8, 48.5, 33.7, 32.7, 32.6, 31.8, 25.4, 24.7, 24.7, 23.9, 23.8. MS (ESI): m/z 620 (M + Na)$^+$, 636 (M + K)$^+$. HRMS (ESI): m/z 598.3279 (M + H)$^+$ (calcd for $C_{36}H_{44}N_3O_5$, 598.3281), 620.3098 (M + Na)$^+$ (calcd for $C_{36}H_{43}N_3NaO_5$, 620.3100). HPLC: purity 96.1%.

Virtual Screening. Virtual screening was performed using Surflex-Dock in Sybyl, version 8.1.1 (Tripos Associates), operating under Red Hat Linux 4.0 with an IBM computer (Intel Pentium 4, 2.8 GHz CPU, and 1 GB memory). The crystallographic structure of CypA and CsA complex (PDB code 1CWA) available from the Protein Data Bank was refined with the structure preparation tool. The 2D structure of approximately 200 000 compounds available in the Asinex database was converted to 3D and minimized with the Tripos force field and Gasteiger−Huckel charge. The binding site was determined in a Protomol file. The binding affinity of the ligands was predicted by five different scoring functions and a consensus score to identify hit 5. After running Surflex-Dock, 20 docked models were selected for each ligand. The best scoring conformer was used to study the binding patterns at the active site. Similar approach was applied during docking to obtain the hypothetical binding mode of the lead **25**. The structure of **25** was drawn into the Sybyl package and was minimized with the

DOI: 10.1021/acs.jmedchem.5b01064
J. Med. Chem. XXXX, XXX, XXX−XXX

Tripos force field and Gasteiger−Huckel charge and was used instead of a library of compounds.

Cell-Based Anti-HCV and MTT Assays. An infectious recombinant isolate derived from a genotype 2a HCV clone (JFH1) JFH1-RLuc was prepared by in vitro transcription of its viral RNA from the cognate plasmid pJFH1-Luc (a gift from Dr. Xulin Chen, Wuhan Institute of Virology, China). In vitro transcripts were electroporated into Huh7.5 cells as previously described.[36,37] This system was designed to examine the efficiency of viral infection and replication by measuring *Renilla* luciferase (RLuc) activity. Naive Huh7.5 cells (grown to 70% confluence) were seeded onto 48-well plates and were either mock-infected with culture medium [Dulbecco's modified Eagle medium (DMEM; Invitrogen, Carlsbad, CA, USA) supplemented with 10% fetal bovine serum (Invitrogen)] or infected with the JFH1-Luc virus at a multiplicity of infection (MOI) of 0.004 for 5 h at 37 °C in the absence or presence of serially (3-fold) diluted test chemicals. On day 3 postinfection, JFH1-Luc-infected and chemical-treated cells were lysed and the EC_{50} were calculated by measuring *Renilla* luciferase activity (*Renilla* luciferase assay system; Promega, Madison, WI, USA). In parallel, the viability of mock-infected and chemical-treated Huh7.5 cells was tested by an MTT (3-(4,5-dimethylthiazol-2-yl)-2,5-diphenyltetrazoliumbromide) (Sigma-Aldrich) assay and the CC_{50} values were calculated as previously described.[38]

Surface Plasmon Resonance. The direct target binding of **25** or CsA was assessed using a dual channel SPR instrument (Reichert, Depew, NY, USA). CypA protein was immobilized to the sensor chip surface via free amine coupling by injecting a mixture of 0.1 M 1-ethyl-3-(3-dimethylaminopropyl)carbodiimide hydrochloride and 0.05 M *N*-hydroxysuccinimide followed by quenching of the remaining activated carboxyl groups with 1 M ethanolamine, pH 8.5. A second reference cell was treated similarly, but the target protein was excluded. All working peptide dilutions were prepared in running buffer (PBS with 0.2% DMSO) and were injected for 3 min (association time) at a flow rate of 30 μL/min followed by a dissociation phase of 3 min. Nonspecific background binding was subtracted from each sensogram using the SPR V4017 data acquisition and alignment program (Reichert, Depew, NY, USA). The binding rates and constants were independent of the flow rate over a wide range. Best-fit kinetic parameters were obtained by global fitting analysis using Scrubber2 (BioLogic Software, Campbell, ACT, Australia).

Calcineurin Phosphatase Assay. Calcium-dependent calcineurin activity was determined by measuring the dephosphorylation of the RII phosphopeptide using a calcineurin cellular activity assay kit (Enzo Life Sciences, Plymouth Meeting, PA, USA). Splenocytes (2×10^6 cells/well) were incubated with CsA or **25** for 20 h and either were left untreated or were stimulated with 1 μg/mL ionomycin (Calbiochem, La Jolla, CA, USA) for an additional 4 h. The cells were subsequently used to measure calcineurin activity.

NFAT Dephosphorylation by Western Blot and Immunofluorescence. Mouse splenocytes (2×10^6 cells/well) were cultured and treated with CsA or **25** for 20 h at 37 °C followed by another 4 h of stimulation with 1 μg/mL ionomycin (Calbiochem, La Jolla, CA, USA). After stimulation, the cells were washed once with sterile PBS, suspended in lysis buffer (Invitrogen, Carlsbad, CA, USA), and incubated on ice for 10 min followed by centrifugation at 19 000*g* for 15 min. The phosphorylation status of NFAT proteins in the supernatant was evaluated by Western blot using a monoclonal anti-NFATc1 antibody (Abcam, Cambridge, MA, USA). To identify the localization of NFAT1 by confocal microscope, the cells were washed and fixed using 3.7% formaldehyde for 20 min at rt after treatment. Thereafter, the cells were washed three times with PBS and were permeabilized using 0.5% Triton X-100 in PBS and were washed again three times with PBS prior to an overnight incubation (4 °C) with a primary antibody at a dilution of 1:100 in PBS containing 3% BSA. After incubation, the cells were again washed twice with PBS and were incubated with an Alexa 546-conjugated secondary antibody (Invitrogen, Carlsbad, CA, USA) diluted 1:200 in PBS containing 3% BSA for 2 h in the dark at rt. The cells were washed two more times in PBS and were counterstained with DAPI (4′,6′-diamidino-2-phenylindole) for 10 min. The cells were washed again with PBS and mounted on glass slides using a coverslip and mounting solution (VectaMount; Vector Laboratories, Inc., Burlingame, CA, USA). The images were captured using a Zeiss confocal laser scanning microscope (Zeiss, Oberkochen, Germany).

Determination of the IL-2 Concentration by ELISA. Spleen cells (2×10^6 cells/well) were seeded in a 24-well plate and were stimulated with ionomycin (1 μg/mL) followed by CsA or **25** treatment in a dose-dependent manner for 24 h at 37 °C. After incubation, the culture media from triplicate wells were pooled and were assayed to determine the IL-2 concentration by ELISA according to a protocol from Enzo Life Sciences (Plymouth Meeting, PA). The IL-2 concentrations were calculated based on IL-2 standards and solutions.

Preparation of the Membrane Fraction. Cells at a confluence of ∼80% in a 10 cm diameter culture dish were scraped using PBS. The cells were pelleted by centrifugation at 220*g* for 10 min. The pellet was resuspended in 1 mL of hypotonic buffer (10 mM Tris-HCl (pH 7.5), 10 mM KCl, 1.5 mM $MgCl_2$, 0.5 mM phenylmethylsulfonyl fluoride (PMSF), and 2 μg/mL leupeptin) and was incubated for 10 min at 4 °C. The suspension was homogenized with 75 strokes using a glass dounce homogenizer and a tight-fitting pestle (Sigma-Aldrich, St. Louis, MO, USA). The nuclei and nondisrupted cells were removed by centrifugation at 220*g* for 10 min at 4 °C. The intracellular membranes in the resulting supernatant were centrifuged immediately at 68 000*g* in a microultracentrifuge (Hitachi, Japan) for 1 h at 4 °C. After centrifugation, the crude replication complex fraction was recovered and used for Western blot analysis.

Real-Time Image Analysis. Huh7 replicon cells expressing a NS5A-GFP fusion protein were plated at 2×10^3 cells/well in 40 μL of culture media in 384-well plates (Greiner Bio-One, μClear black). After incubation overnight, serially diluted compounds in 20 μL of culture media were added. At 72 h postinfection, the plates were fixed with 2% paraformaldehyde (PFA) and the nuclei were stained with 10 μg/mL Hoechst 33342 (Sigma-Aldrich, St. Louis, MO, USA). The cells were visualized by fully automated confocal microscopy (Opera, PerkinElmer) and were analyzed with an in-house written software program. The infected cells were measured by their GFP expression, and cytotoxicity was measured by counting the nuclei. The EC_{50} and CC_{50} were calculated by nonlinear regression using GraphPad Prism (GraphPad Software, Inc., La Jolla, CA, USA).

Real-Time Quantitative Reverse Transcriptase PCR Analysis. Real-time quantitative reverse transcriptase PCR (qRT-PCR) was performed using the SYBR Green PCR Master Mix (Invitrogen/Applied Biosystems, Carlsbad, CA, USA) and the ABI Prism 7300 real-time PCR system (Applied Biosystems, Carlsbad, CA, USA) according to the manufacturer's instructions. Calculations based on the $2^{-\Delta\Delta C_T}$ method were performed using the following equation: R (ratio) = $2^{-[\Delta C_T(\text{sample}) - \Delta C_T(\text{control})]}$. The data were expressed as the fold change in the treatment groups relative to that in the controls and were normalized to GAPDH.

Determination of IL-8 and IFN-α Concentrations in the Cell Culture Media Using ELISA. HCV replicon Con1b cells (2×10^6 cells/well) were plated in 6-well plates followed by treatment with 2 μM CsA or **25** in a time-dependent manner for up to 4 days at 37 °C. After incubation, the culture media were pooled and assayed for IL-8 and IFN-α concentrations using ELISA (eBioscience, San Diego, CA, USA) per the manufacturer's instructions.

Synergy Analysis. To determine whether the effects of the combination of **25** with IFN-α, ribavirin, or telaprevir were synergistic, additive, or antagonistic, the calcuSyn software (Biosoft, Cambridge, U.K.) was used to calculate the combination index (CI) value. Additivity, synergy, and antagonism were indicated by CI = 1.0, <1.0, and >1.0, respectively.

HCV Mouse Model. Immunodeficient, 5- to 6-week-old NOD/SCID female mice (Charles River Laboratories, USA) were used in the in vivo experiments. Animal use and the experimental protocol (KHUASP (SE)-11-045) were approved by the Institutional Animal Care and Use Committee of Kyung Hee University (Seoul, Korea). The mice were engrafted with control Huh7 cells or Huh7 cells containing the HCV-Con1b replicon (1×10^6 cells in 200 μL of PBS)

DOI: 10.1021/acs.jmedchem.5b01064
J. Med. Chem. XXXX, XXX, XXX−XXX

by intrasplenic injection.[49] The cell transplantation and surgical procedures were performed under anesthesia with prophylactic antibiotics. Intraperitoneal administration of CsA and **25** (50 mg/kg) was started 6 weeks after the cell transplantation and was continued for 14 days. Each treatment group consisted of five animals. After treatment completion, the mice were euthanized and the liver tissue was dissected for analysis.

Histology and Fluorescence Immunohistochemistry. The liver tissue of each mouse was dissected and cryoprotected in 30% sucrose for the subsequent preparation of paraffin-embedded tissue sections. The paraffin tissue sections were prepared for H&E staining. The deparaffinized and rehydrated sections were incubated overnight at 4 °C with a monoclonal antibody against human hepatocytes (Hep par 1) and HCV NS5A (Santa Cruz Biotechnologies, Inc., Santa Cruz, CA, USA) at a 1:50 dilution. After three washes, the sections were incubated with an Alexa Fluor 488- or Alexa Fluor 546-conjugated anti-rabbit or anti-mouse IgG antibody (Invitrogen, Carlsbad, CA, USA) at a dilution of 1:100 for 2 h. The nuclei were labeled with DAPI for 5 min. Images were acquired using confocal microscopy.

Western Blot Analysis. The cell extracts were separated by SDS−PAGE and were transferred onto a nitrocellulose membrane. After blocking, the membranes were incubated with primary antibodies followed by incubation with a secondary antibody. The protein samples were detected with enhanced chemiluminescence reagents (Santa Cruz Biotechnology, Inc., Santa Cruz, CA, USA).

■ ASSOCIATED CONTENT

Ⓢ Supporting Information

The Supporting Information is available free of charge on the ACS Publications website at DOI: 10.1021/acs.jmedchem.5b01064.

Molecular formula strings (CSV)

Synthesis and characterization of the compounds, molecular docking, and details of the biological assays (PDF)

■ AUTHOR INFORMATION

Corresponding Authors

*S.S.K.: phone, +82-2-961-0524; fax, +82-2-959-8168; e-mail, sgskim@khu.ac.kr.

*W.-J.C.: phone, +82-62-530-2933; fax, +82-62-530-2911; e-mail, wjcho@jnu.ac.kr.

Present Address

[▽]S.Y.: Department of Medicinal Chemistry, College of Pharmacy, Translational Oncology Program, University of Michigan, North Campus Research Complex, Building 520, Ann Arbor, MI 48109, U.S.

Author Contributions

[○]S.Y. and J.K.R. contributed equally.

Notes

The authors declare no competing financial interest.

■ ACKNOWLEDGMENTS

This work was supported by a grant from the National Research Foundation of Korea (NRF) funded by the Korean government (MEST) (Grant 2011-0030072) and Korea Health Industry Development Institute (KHIDI) (Grant HI12C1640).

■ ABBREVIATIONS USED

DAA, direct-acting antiviral; IFN-α, interferon α; CypA, cyclophilin A; CsA, cyclosporin A; PPIase, peptidylprolyl cis−trans isomerase; NFAT, nuclear factor of activated T cell; TFE, 2,2,2-trifluoroethanol; IL-2, interleukin 2; K_D, dissociation constant; ITC, isothermal titration calorimetry; Janus kinase-signal transducer and activator of transcription (JAK-STAT); ISG, IFN-stimulated gene

■ REFERENCES

(1) Seeff, L. B. Natural history of hepatitis C. *Hepatology* **1997**, *26*, 21S−28S.

(2) Kowdley, K. V. Hematologic side effects of interferon and ribavirin therapy. *J. Clin. Gastroenterol.* **2005**, *39*, S3−8.

(3) Strader, D. B.; Seeff, L. B. A brief history of the treatment of viral hepatitis C. *Clin. Liver Dis.* **2012**, *1*, 6−11.

(4) Heim, M. H. 25 years of interferon-based treatment of chronic hepatitis C: an epoch coming to an end. *Nat. Rev. Immunol.* **2013**, *13*, 535−542.

(5) Liang, T. J.; Ghany, M. G. Current and future therapies for hepatitis C virus infection. *N. Engl. J. Med.* **2013**, *368*, 1907−1917.

(6) Manns, M. P.; von Hahn, T. Novel therapies for hepatitis C - one pill fits all? *Nat. Rev. Drug Discovery* **2013**, *12*, 595−610.

(7) Sherman, K. E.; Flamm, S. L.; Afdhal, N. H.; Nelson, D. R.; Sulkowski, M. S.; Everson, G. T.; Fried, M. W.; Adler, M.; Reesink, H. W.; Martin, M.; Sankoh, A. J.; Adda, N.; Kauffman, R. S.; George, S.; Wright, C. I.; Poordad, F. Response-guided telaprevir combination treatment for hepatitis C virus infection. *N. Engl. J. Med.* **2011**, *365*, 1014−1024.

(8) Bacon, B. R.; Gordon, S. C.; Lawitz, E.; Marcellin, P.; Vierling, J. M.; Zeuzem, S.; Poordad, F.; Goodman, Z. D.; Sings, H. L.; Boparai, N.; Burroughs, M.; Brass, C. A.; Albrecht, J. K.; Esteban, R. Boceprevir for previously treated chronic HCV genotype 1 infection. *N. Engl. J. Med.* **2011**, *364*, 1207−1217.

(9) Yau, A. H.; Yoshida, E. M. Hepatitis C drugs: the end of the pegylated interferon era and the emergence of all-oral interferon-free antiviral regimens: a concise review. *Can. J. Gastroenterol. Hepatol.* **2014**, *28*, 445−451.

(10) Wyles, D.; Pockros, P.; Morelli, G.; Younes, Z.; Svarovskaia, E.; Yang, J. C.; Pang, P. S.; Zhu, Y.; McHutchison, J. G.; Flamm, S.; Lawitz, E. Ledipasvir-sofosbuvir plus ribavirin for patients with genotype 1 hepatitis C virus previously treated in clinical trials of sofosbuvir regimens. *Hepatology* **2015**, *61*, 1793−1797.

(11) Lalezari, J.; Sullivan, J. G.; Varunok, P.; Galen, E.; Kowdley, K. V.; Rustgi, V.; Aguilar, H.; Felizarta, F.; McGovern, B.; King, M.; Polepally, A. R.; Cohen, D. E. Ombitasvir/paritaprevir/r and dasabuvir plus ribavirin in HCV genotype 1-infected patients on methadone or buprenorphine. *J. Hepatol.* **2015**, *63*, 364−369.

(12) Chayama, K.; Notsumata, K.; Kurosaki, M.; Sato, K.; Rodrigues, L., Jr.; Setze, C.; Badri, P.; Pilot-Matias, T.; Vilchez, R. A.; Kumada, H. Randomized trial of interferon- and ribavirin-free ombitasvir/paritaprevir/ritonavir in treatment-experienced hepatitis C virus-infected patients. *Hepatology* **2015**, *61*, 1523−1532.

(13) Jacobson, I. M.; Gordon, S. C.; Kowdley, K. V.; Yoshida, E. M.; Rodriguez-Torres, M.; Sulkowski, M. S.; Shiffman, M. L.; Lawitz, E.; Everson, G.; Bennett, M.; Schiff, E.; Al-Assi, M. T.; Subramanian, G. M.; An, D.; Lin, M.; McNally, J.; Brainard, D.; Symonds, W. T.; McHutchison, J. G.; Patel, K.; Feld, J.; Pianko, S.; Nelson, D. R. Sofosbuvir for hepatitis C genotype 2 or 3 in patients without treatment options. *N. Engl. J. Med.* **2013**, *368*, 1867−1877.

(14) Nelson, D. R.; Cooper, J. N.; Lalezari, J. P.; Lawitz, E.; Pockros, P. J.; Gitlin, N.; Freilich, B. F.; Younes, Z. H.; Harlan, W.; Ghalib, R.; Oguchi, G.; Thuluvath, P. J.; Ortiz-Lasanta, G.; Rabinovitz, M.; Bernstein, D.; Bennett, M.; Hawkins, T.; Ravendhran, N.; Sheikh, A. M.; Varunok, P.; Kowdley, K. V.; Hennicken, D.; McPhee, F.; Rana, K.; Hughes, E. A. All-oral 12-week treatment with daclatasvir plus sofosbuvir in patients with hepatitis C virus genotype 3 infection: ALLY-3 phase III study. *Hepatology* **2015**, *61*, 1127−1135.

(15) Ruane, P. J.; Ain, D.; Stryker, R.; Meshrekey, R.; Soliman, M.; Wolfe, P. R.; Riad, J.; Mikhail, S.; Kersey, K.; Jiang, D.; Massetto, B.; Doehle, B.; Kirby, B. J.; Knox, S. J.; McHutchison, J. G.; Symonds, W. T. Sofosbuvir plus ribavirin for the treatment of chronic genotype 4 hepatitis C virus infection in patients of Egyptian ancestry. *J. Hepatol.* **2015**, *62*, 1040−1046.

DOI: 10.1021/acs.jmedchem.5b01064
J. Med. Chem. XXXX, XXX, XXX−XXX

(16) European Association for the Study of Liver.. EASL Recommendations on Treatment of Hepatitis C 2015. *J. Hepatol.* **2015**, *63*, 199−236.
(17) Poveda, E.; Wyles, D. L.; Mena, A.; Pedreira, J. D.; Castro-Iglesias, A.; Cachay, E. Update on hepatitis C virus resistance to direct-acting antiviral agents. *Antiviral Res.* **2014**, *108*, 181−191.
(18) Wyles, D. L. Beyond telaprevir and boceprevir: resistance and new agents for hepatitis C virus infection. *Top. Antiviral Med.* **2012**, *20*, 139−145.
(19) Pawlotsky, J. M. Treatment failure and resistance with direct-acting antiviral drugs against hepatitis C virus. *Hepatology* **2011**, *53*, 1742−1751.
(20) Xiao, F.; Fofana, I.; Heydmann, L.; Barth, H.; Soulier, E.; Habersetzer, F.; Doffoel, M.; Bukh, J.; Patel, A. H.; Zeisel, M. B.; Baumert, T. F. Hepatitis C virus cell-cell transmission and resistance to direct-acting antiviral agents. *PLoS Pathog.* **2014**, *10*, e1004128.
(21) Aissa Larousse, J.; Trimoulet, P.; Recordon Pinson, P.; Tauzin, B.; Azzouz, M. M.; Ben Mami, N.; Cheikh, I.; Triki, H.; Fleury, H. Prevalence of hepatitis C virus (HCV) variants resistant to NS5A inhibitors in naive patients infected with HCV genotype 1 in Tunisia. *Virol. J.* **2015**, *12*, 84.
(22) Tong, X.; Le Pogam, S.; Li, L.; Haines, K.; Piso, K.; Baronas, V.; Yan, J. M.; So, S. S.; Klumpp, K.; Najera, I. In vivo emergence of a novel mutant L159F/L320F in the NS5B polymerase confers low-level resistance to the HCV polymerase inhibitors mericitabine and sofosbuvir. *J. Infect. Dis.* **2014**, *209*, 668−675.
(23) Shi, N.; Hiraga, N.; Imamura, M.; Hayes, C. N.; Zhang, Y.; Kosaka, K.; Okazaki, A.; Murakami, E.; Tsuge, M.; Abe, H.; Aikata, H.; Takahashi, S.; Ochi, H.; Tateno-Mukaidani, C.; Yoshizato, K.; Matsui, H.; Kanai, A.; Inaba, T.; McPhee, F.; Gao, M.; Chayama, K. Combination therapies with NS5A, NS3 and NS5B inhibitors on different genotypes of hepatitis C virus in human hepatocyte chimeric mice. *Gut* **2013**, *62*, 1055−1061.
(24) Watashi, K.; Hijikata, M.; Hosaka, M.; Yamaji, M.; Shimotohno, K. Cyclosporin A suppresses replication of hepatitis C virus genome in cultured hepatocytes. *Hepatology* **2003**, *38*, 1282−1288.
(25) Chatterji, U.; Bobardt, M.; Selvarajah, S.; Yang, F.; Tang, H.; Sakamoto, N.; Vuagniaux, G.; Parkinson, T.; Gallay, P. The isomerase active site of cyclophilin A is critical for hepatitis C virus replication. *J. Biol. Chem.* **2009**, *284*, 16998−17005.
(26) Kaul, A.; Stauffer, S.; Berger, C.; Pertel, T.; Schmitt, J.; Kallis, S.; Zayas, M.; Lohmann, V.; Luban, J.; Bartenschlager, R. Essential role of cyclophilin A for hepatitis C virus replication and virus production and possible link to polyprotein cleavage kinetics. *PLoS Pathog.* **2009**, *5*, e1000546.
(27) Liu, J. O. Calmodulin-dependent phosphatase, kinases, and transcriptional corepressors involved in T-cell activation. *Immunol. Rev.* **2009**, *228*, 184−198.
(28) Goto, K.; Watashi, K.; Murata, T.; Hishiki, T.; Hijikata, M.; Shimotohno, K. Evaluation of the anti-hepatitis C virus effects of cyclophilin inhibitors, cyclosporin A, and NIM811. *Biochem. Biophys. Res. Commun.* **2006**, *343*, 879−884.
(29) Hopkins, S.; Scorneaux, B.; Huang, Z.; Murray, M. G.; Wring, S.; Smitley, C.; Harris, R.; Erdmann, F.; Fischer, G.; Ribeill, Y. SCY-635, a novel nonimmunosuppressive analog of cyclosporine that exhibits potent inhibition of hepatitis C virus RNA replication in vitro. *Antimicrob. Agents Chemother.* **2010**, *54*, 660−672.
(30) Paeshuyse, J.; Kaul, A.; De Clercq, E.; Rosenwirth, B.; Dumont, J. M.; Scalfaro, P.; Bartenschlager, R.; Neyts, J. The non-immunosuppressive cyclosporin DEBIO-025 is a potent inhibitor of hepatitis C virus replication in vitro. *Hepatology* **2006**, *43*, 761−770.
(31) Zydowsky, L. D.; Etzkorn, F. A.; Chang, H. Y.; Ferguson, S. B.; Stolz, L. A.; Ho, S. I.; Walsh, C. T. Active site mutants of human cyclophilin A separate peptidyl-prolyl isomerase activity from cyclosporin A binding and calcineurin inhibition. *Protein Sci.* **1992**, *1*, 1092−1099.
(32) Davis, T. L.; Walker, J. R.; Campagna-Slater, V.; Finerty, P. J.; Paramanathan, R.; Bernstein, G.; MacKenzie, F.; Tempel, W.; Ouyang, H.; Lee, W. H.; Eisenmesser, E. Z.; Dhe-Paganon, S. Structural and biochemical characterization of the human cyclophilin family of peptidyl-prolyl isomerases. *PLoS Biol.* **2010**, *8*, e1000439.
(33) Mikol, V.; Kallen, J.; Pflugl, G.; Walkinshaw, M. D. X-ray structure of a monomeric cyclophilin A-cyclosporin A crystal complex at 2.1 A resolution. *J. Mol. Biol.* **1993**, *234*, 1119−1130.
(34) Ngouansavanh, T.; Zhu, J. Alcohols in isonitrile-based multicomponent reaction: Passerini reaction of alcohols in the presence of o-iodoxybenzoic acid. *Angew. Chem., Int. Ed.* **2006**, *45*, 3495−3497.
(35) Domling, A. Recent developments in isocyanide based multicomponent reactions in applied chemistry. *Chem. Rev.* **2006**, *106*, 17−89.
(36) Borawski, J.; Troke, P.; Puyang, X.; Gibaja, V.; Zhao, S.; Mickanin, C.; Leighton-Davies, J.; Wilson, C. J.; Myer, V.; Cornellataracido, I.; Baryza, J.; Tallarico, J.; Joberty, G.; Bantscheff, M.; Schirle, M.; Bouwmeester, T.; Mathy, J. E.; Lin, K.; Compton, T.; Labow, M.; Wiedmann, B.; Gaither, L. A. Class III phosphatidylinositol 4-kinase alpha and beta are novel host factor regulators of hepatitis C virus replication. *J. Virol.* **2009**, *83*, 10058−10074.
(37) Wu, Y.; Liao, Q.; Yang, R.; Chen, X. A novel luciferase and GFP dual reporter virus for rapid and convenient evaluation of hepatitis C virus replication. *Virus Res.* **2011**, *155*, 406−414.
(38) Jang, Y. J.; Achary, R.; Lee, H. W.; Lee, H. J.; Lee, C. K.; Han, S. B.; Jung, Y. S.; Kang, N. S.; Kim, P.; Kim, M. Synthesis and anti-influenza virus activity of 4-oxo- or thioxo-4,5-dihydrofuro[3,4-c]pyridin-3(1H)-ones. *Antiviral Res.* **2014**, *107*, 66−75.
(39) Kim, O. H.; Kim, Y. O.; Shim, J. H.; Jung, Y. S.; Jung, W. J.; Choi, W. C.; Lee, H.; Lee, S. J.; Kim, K. K.; Auh, J. H.; Kim, H.; Kim, J. W.; Oh, T. K.; Oh, B. C. beta-propeller phytase hydrolyzes insoluble Ca(2+)-phytate salts and completely abrogates the ability of phytate to chelate metal ions. *Biochemistry* **2010**, *49*, 10216−10227.
(40) Chow, C. W.; Rincon, M.; Davis, R. J. Requirement for transcription factor NFAT in interleukin-2 expression. *Mol. Cell. Biol.* **1999**, *19*, 2300−2307.
(41) Hopkins, S.; Gallay, P. Cyclophilin inhibitors: an emerging class of therapeutics for the treatment of chronic hepatitis C infection. *Viruses* **2012**, *4*, 2558−2577.
(42) Kaufmann, Y.; Chang, A. E.; Robb, R. J.; Rosenberg, S. A. Mechanism of action of cyclosporin A: inhibition of lymphokine secretion studied with antigen-stimulated T cell hybridomas. *J. Immunol.* **1984**, *133*, 3107−3111.
(43) Hopkins, S.; Bobardt, M.; Chatterji, U.; Garcia-Rivera, J. A.; Lim, P.; Gallay, P. A. The cyclophilin inhibitor SCY-635 disrupts hepatitis C virus NS5A-cyclophilin A complexes. *Antimicrob. Agents Chemother.* **2012**, *56*, 3888−3897.
(44) Foster, T. L.; Gallay, P.; Stonehouse, N. J.; Harris, M. Cyclophilin A interacts with domain II of hepatitis C virus NS5A and stimulates RNA binding in an isomerase-dependent manner. *J. Virol.* **2011**, *85*, 7460−7464.
(45) Blight, K. J.; Kolykhalov, A. A.; Rice, C. M. Efficient initiation of HCV RNA replication in cell culture. *Science* **2000**, *290*, 1972−1974.
(46) Kumthip, K.; Chusri, P.; Jilg, N.; Zhao, L.; Fusco, D. N.; Zhao, H.; Goto, K.; Cheng, D.; Schaefer, E. A.; Zhang, L.; Pantip, C.; Thongsawat, S.; O'Brien, A.; Peng, L. F.; Maneekarn, N.; Chung, R. T.; Lin, W. Hepatitis C virus NS5A disrupts STAT1 phosphorylation and suppresses type I interferon signaling. *J. Virol.* **2012**, *86*, 8581−8591.
(47) Zimmermann, H. W.; Seidler, S.; Gassler, N.; Nattermann, J.; Luedde, T.; Trautwein, C.; Tacke, F. Interleukin-8 is activated in patients with chronic liver diseases and associated with hepatic macrophage accumulation in human liver fibrosis. *PLoS One* **2011**, *6*, e21381.
(48) Flisiak, R.; Feinman, S. V.; Jablkowski, M.; Horban, A.; Kryczka, W.; Pawlowska, M.; Heathcote, J. E.; Mazzella, G.; Vandelli, C.; Nicolas-Metral, V.; Grosgurin, P.; Liz, J. S.; Scalfaro, P.; Porchet, H.; Crabbe, R. The cyclophilin inhibitor Debio 025 combined with PEG IFNalpha2a significantly reduces viral load in treatment-naive hepatitis C patients. *Hepatology* **2009**, *49*, 1460−1468.

DOI: 10.1021/acs.jmedchem.5b01064
J. Med. Chem. XXXX, XXX, XXX−XXX

(49) Pan, Q.; Ramakrishnaiah, V.; Henry, S.; Fouraschen, S.; de Ruiter, P. E.; Kwekkeboom, J.; Tilanus, H. W.; Janssen, H. L.; van der Laan, L. J. Hepatic cell-to-cell transmission of small silencing RNA can extend the therapeutic reach of RNA interference (RNAi). *Gut* **2012**, *61*, 1330−1339.

DOI: 10.1021/acs.jmedchem.5b01064
J. Med. Chem. XXXX, XXX, XXX−XXX